THE
ENGLISH ELECTRIC
JOURNAL

VOLUME THIRTEEN • NUMBER SIX • JUNE 1954

THE ENGLISH ELECTRIC JOURNAL

VOLUME THIRTEEN NUMBER SIX JUNE 1954

CONTENTS

Page 223 : HYDRO-ELECTRIC DEVELOPMENT IN PORTUGAL (PART I).

240 : THE NAPIER DIFFERENTIAL PRESSURE GAUGES.

243 : THE FLOW OF POWER AND REACTIVE COMPONENTS IN RECTIFIER AND INVERTER EQUIPMENTS (PART II), *by T. E. Calverley, B.Sc., A.M.I.E.E., Chief Engineer, Rectifier Department.*

260 : THE PROPERTY OF NON-DETERIORATION IN THE 'ENGLISH ELECTRIC' H.R.C. FUSE LINK, *by E. Jacks, A.M.I.E.E., Fusegear Section.*

All communications respecting Editorial Contents should be addressed to The Editor, THE ENGLISH ELECTRIC JOURNAL, THE ENGLISH ELECTRIC COMPANY LIMITED, STAFFORD, ENGLAND.

The dam and power station at Castelo do Bode on the River Zezere in Portugal, with the spillway and one of the disperser valves discharging simultaneously

Hydro-Electric Development in Portugal

This description is abridged from the article published in 'The Engineer' of October 30th and November 6th, 13th and 20th, 1953.

PART ONE

Portugal possesses few natural resources, and the steady advancement in industrialisation since the end of the world war of what is still predominantly an agricultural country is therefore all the more remarkable. Like other Western nations, Portugal was hampered by financial difficulties after the war, but much progress has been made. The Government recognised that without greater industrialisation little could be done to raise the general standard of living, and that cheap and abundant power was essential for the establishment of basic industries. Although deficient in coal, Portugal is fortunate in her rivers, which provide a vast potential power, and some ten years ago an ambitious plan of hydro-electric development was prepared. Shortage of gold reserves and foreign currency have delayed some of the works, but despite these handicaps much has been done with available resources, and British engineers and manufacturing facilities have been able to play a useful part.

In 1944 two laws were enacted by the Portuguese Government, one concerned with the reorganisation of industrial development and the other with the electrification of the country. In 1945 three companies were created, namely, the Hidro-Electrica do Zezere, the Hidro-Electrica do Cavado, and the Companhia Nacional de Electricidade—

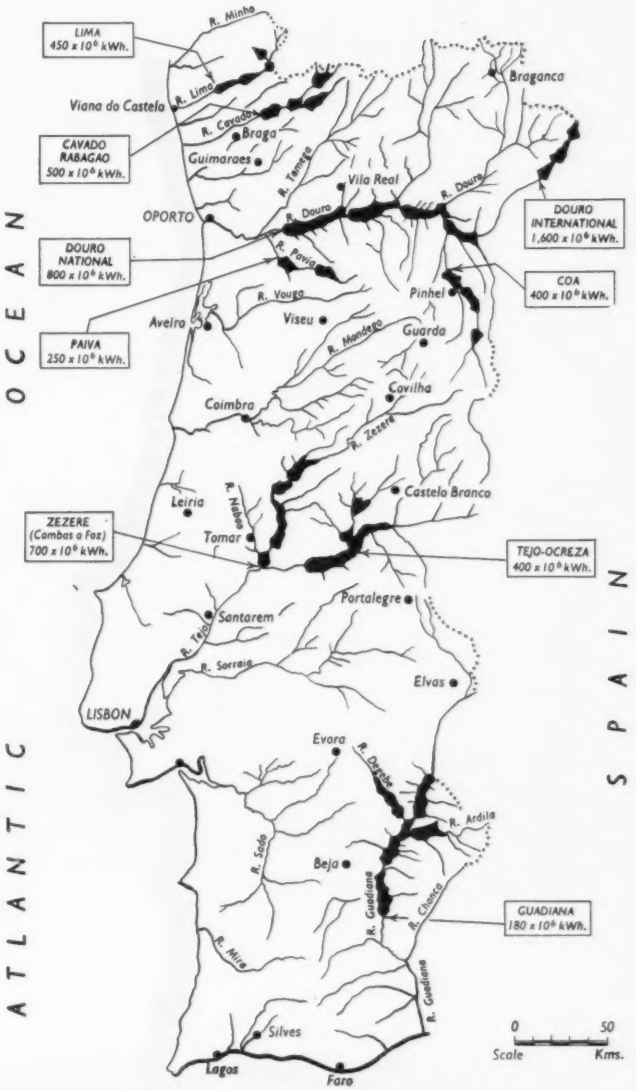

Fig. 1.
Map of Portuguese hydro-electric projects

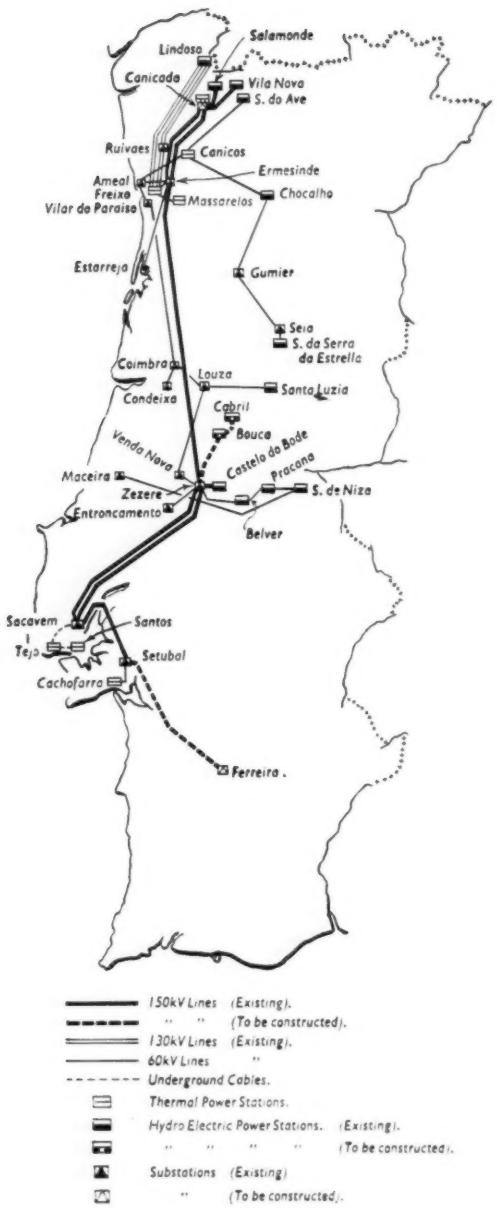

Fig. 2.—Distribution system

the first two to produce electrical energy in the central and northern parts of the country respectively, and the third to transmit this energy to the centres of demand. Because of the important part which these enterprises were destined to play in the national economy, the government participated substantially in their finance and administration, but complete nationalisation was avoided and the companies retained their private standing.

Before the formation of these undertakings, two British companies, the English Electric Export and Trading Company, Ltd., and Metropolitan-Vickers Electrical Export Company, Ltd., acting together, sent an engineering mission to Portugal to confer with the Portuguese engineers who had been appointed to study various hydro-electric projects. These two companies became known in Portugal as the ' British Group.'

The engineering mission collected sufficient data to enable it in 1945 to put forward comprehensive proposals for developing the available water power and, in 1946, after further discussions, the newly-formed Portuguese power companies placed contracts with the ' British Group ' for the supply and erection of hydraulic and electrical plant and equipment for the generating stations at Castelo do Bode on the River Zezere and at Vila Nova on the River Cavado. At a later date a contract was placed with the same group by the Companhia Nacional de Electricidade for the substation at Castelo do Bode, known as the Zezere substation.

Fig. 1 shows the Zezere and Cavado rivers, together with various other hydro-electric projects included in the original plan, some of which are now under construction, and Fig. 2 shows the network of power stations, substations and transmission lines.

The first and largest of the hydro-electric schemes was inaugurated on January 21, 1951, when the then President of the Portuguese Republic, Marshal Carmona, opened the hydro-electric power station at Castelo do Bode. A few months later, on June 10th, Dr. Costa Leite, Minister of the Presidency, representing the President, opened the hydro-electric power station at Vila Nova. The substations constructed by Companhia Nacional de Electricidade, including that at Zezere, were formally inaugurated by the succeeding President, General Lopes, in July, 1952.

RIVER ZEZERE POWER SCHEME

Because of its central geographical position, high rainfall and other favourable conditions, the River

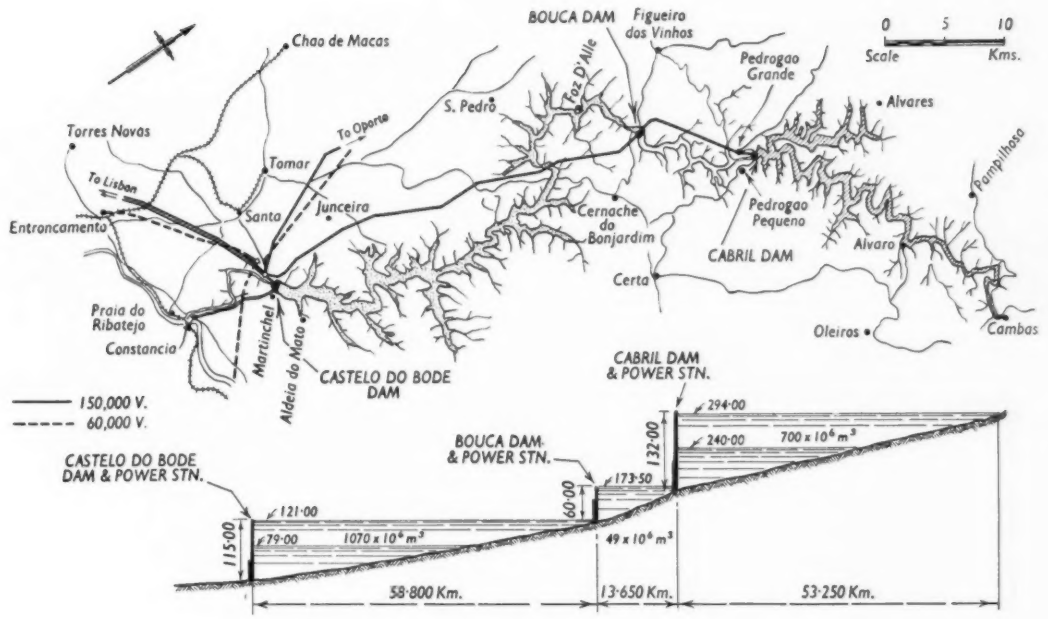

Fig. 3.—Plan and profile of River Zezere development

Zezere was chosen initially as the principal source for the development of hydro-electric power and focal point of the national electric network. The concession granted to the Zezere company comprised the lower course of the river above its junction with the Tagus, having a length of about 140 km (87 miles), and a fall over that length of 275 m (904 ft).

The complete scheme, which is multi-purpose in character, includes the building of dams and the formation of large storage reservoirs which, besides their purely hydro-electric function, will control the present irregular flow of the river, assist irrigation, prevent flood damage, and improve navigation.

The scheme is being carried out in three steps or stages, as shown in the river plan and profile in Fig. 3, and Table I gives the more important characteristics.

Table 1

RIVER ZEZERE POWER SCHEME

Project	Height of dam		Capacity of reservoir		Average head		Installed capacity		Average annual output kWh × 10^6
	Metres	Feet	$m^3 \times 10^6$	Acre-feet	Metres	Feet	No. of units	MVA each	
Cabril	132	433	700	567,000	108	354	2	61	190
Bouca	60	197	49	39,700	54	177	2	28	110
Castelo do Bode	115	377	1,070	867,500	80	262	3	57·4	380

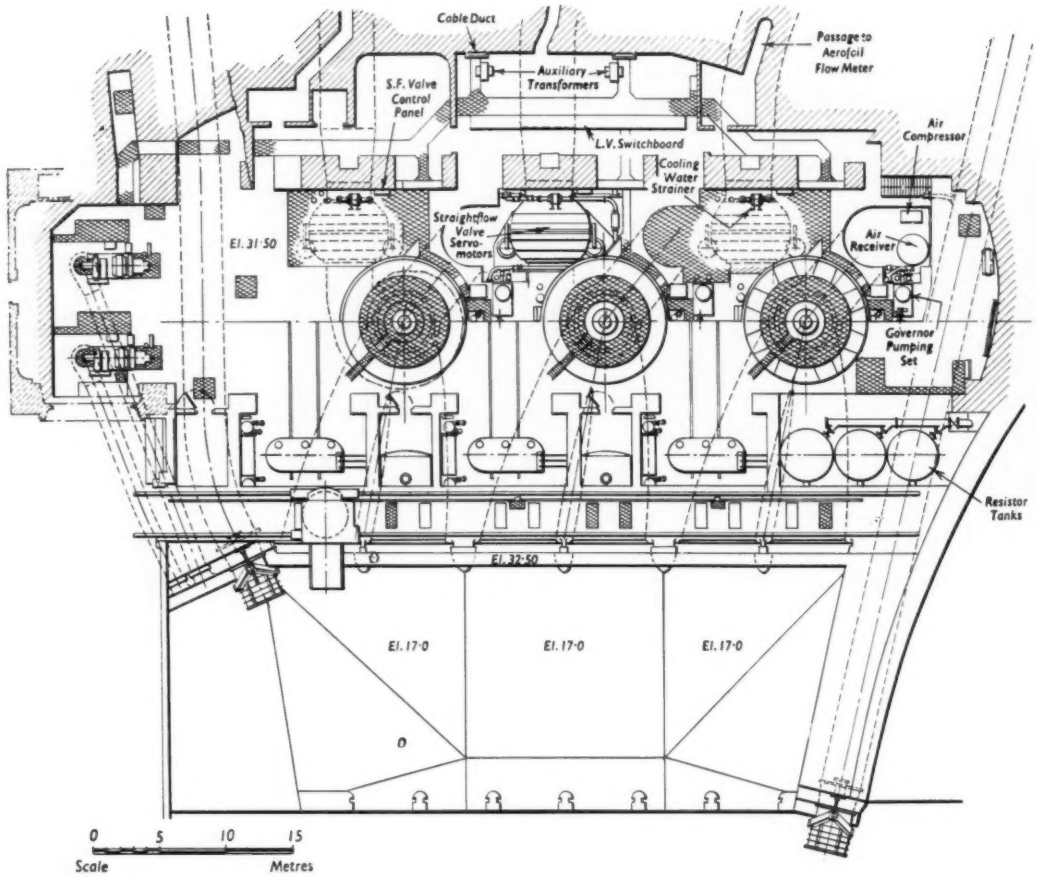

Fig. 4.—Arrangement of Castelo do Bode power station (plan)

The first and third of the above schemes, namely Cabril and Castelo do Bode, were selected for the earliest development, and of these two it was decided to proceed first with Castelo do Bode, owing to the necessity of forming a large reservoir as quickly as possible for securing maximum regulation of the river. The Castelo do Bode dam is one of the largest of its kind in Europe and the storage capacity of the reservoir is only surpassed in the U.S.A. Incorporated in the dam is another important civil engineering work, the flood spillway, designed to deal with a discharge of 4,100 cubic metres (144,790 cubic feet) per second. The power station is equipped with three generating units having a rated total output of 172.2 MVA.

The development at Cabril followed a few years later than Castelo do Bode, and the contract for the power station plant and equipment was again placed with the same 'British Group.' Under a new construction plan approved by the Portuguese Government it is now proposed to proceed with the Bouca project, which figures second in Table I.

CASTELO DO BODE POWER STATION

The principal works at Castelo do Bode, namely, the dam, spillway and power station building (Frontispiece), are very compact in their layout,

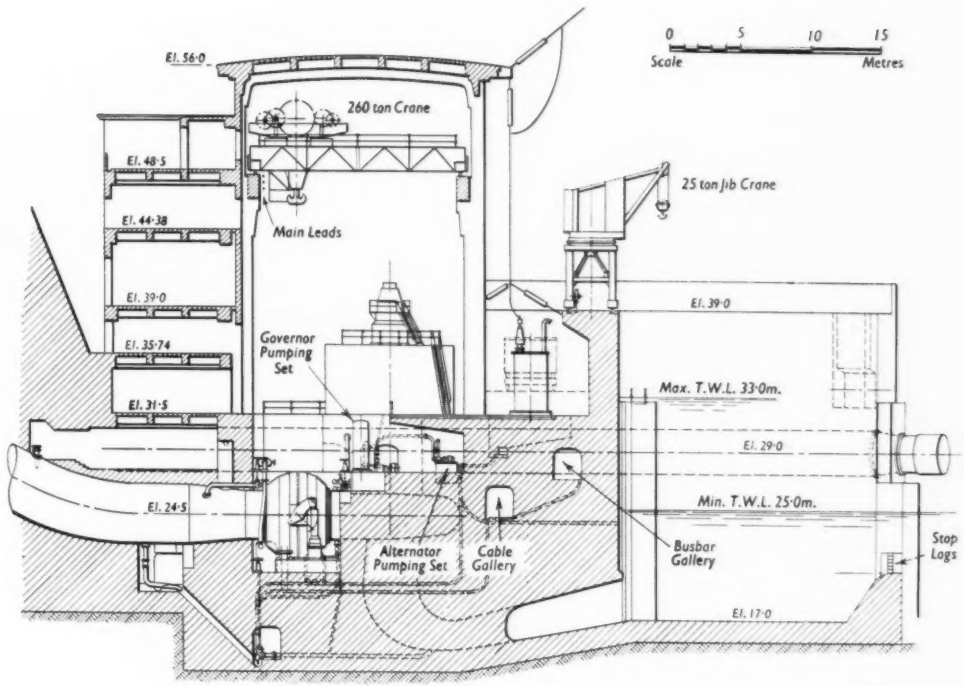

Fig. 5.—Arrangement of Castelo do Bode power station (elevation)

which has simplified construction and promoted economy. The dam, which is of the arch type, was designed to suit the local topographic conditions and it is combined with an artificial abutment of some magnitude on the right bank. The spillway is situated on the dam near the left bank and is quite independent of the power station building. Forced discharge through two large openings was adopted, after it had been found by test that free discharge was impracticable. Regulation of the flow is effected by two sector gates at the outlet of the discharge openings.

The power station was built at the foot of the dam and is in three main sections : first, the machine hall containing the generating units ; secondly, an annexe between machine hall and dam in which there are housed the control gear, various essential services and the administrative offices ; and thirdly, a platform downstream of the machine hall carrying the main transformers and the artificial test loading equipment.

The penstocks for the main and auxiliary turbines are embedded in the dam structure and their intakes on the dam face are provided with detritus screens. Protection is given at the upstream ends of the main penstocks by caterpillar type sluice gates.

There are two 3 m diameter (9 ft 10 in) scour culverts, one on each side of the three machines. They pass through the dam and the power station foundation and terminate in 2·6 m (8 ft 6 in) diameter disperser valves, each capable of discharging 150 cubic metres (150 tons) of water per second under a head of 95 m (312 ft). The design of the valves is such that the energy of this very heavy discharge is dissipated by converting the solid jet into a hollow cone, thus avoiding erosion of the banks of the narrow gorge and the river bed. The valves are arranged for hand and electrical operation by remote control.

Power House

The machine hall is on a single floor which

renders every part of the plant easily accessible and enables all parts to be readily handled by the main crane. In the machine hall are the main generating sets, and next to each set are the governor actuator with its servo-motors, oil pumping set and oil pressure receiver, the bearing coolers, the generator oil pumping set, the field suppression cubicle and the gauge panel. At convenient positions are the air compressor equipment for operation of the generator brakes, the compressor set for lowering the level of the water in the draught tubes when the generators are operating as synchronous condensers, and a sump containing two pumps for dewatering the turbine draught tubes and two drainage pumps.

The three 3·35 m (11 ft 0 in) bore ' Straightflow ' inlet valves for the main turbines are placed beneath the floor level and connect the penstocks with the inlets of the turbine spiral casings. They are readily accessible to the main crane by the removal of chequer plating.

In the annexe upstream of the machine hall is a control gallery which overlooks the generating plant and, beneath it, the cable gallery, workshop and stores and the low voltage switchgear for the A.C. and D.C. auxiliary services. On the platform downstream of the machine hall are the three main transformers with their oil cooling equipment and the two oil reservoirs each containing sufficient oil for one transformer. On the same platform are the three water resistances of the artificial loading equipment used for testing purposes, and at its downstream end a wall has been built for protection against flooding due to abnormal rise in water level. Upon it runs a 25-ton jib crane for handling the draught tube gates and the parts of the disperser valves. Beneath the platform there are two galleries housing the 15 kV busbars and the control cables. Copper connections are taken from the 165 kV terminals of the main step-up transformers to the roof of the power station from which there are short overhead lines to the Zezere substation. This is situated on a plateau about 800 m from the power station.

Drawings of the power station, in plan and part section respectively, are shown in Figs. 4 and 5, and an interior view of the power station in Fig. 6.

Fig. 6.—Three 73,000 h.p. generating sets at Castelo do Bode

Turbines

The three main turbines are vertical shaft reaction machines, designed to give an output of 73,000 h.p. under a maximum net head of 95 m (317 ft), and 62,000 h.p. under an average net head of 80 m (262 ft). The discharges under these conditions are 65·8 cubic metres (2,323 cubic feet) per second and 66·3 cubic metres (2,340 cubic feet) per second respectively. The headwater level under normal conditions of operation varies between 79 m (259 ft) and 122 m (400 ft), and the tailwater level between 23·50 m (77 ft) and 25 m (82 ft). Under exceptional flood conditions the tailwater can attain a height of 32·50 m (107 ft).

The normal speed of the turbines is 214 r.p.m. and their runaway speed under maximum head will not exceed 400 r.p.m. The resulting specific speed of the runner, which is quite high for the operating head, is made possible by accurate design and streamline finish of the runner vanes and the sufficiently low setting of the turbines.

In the construction of the turbines much use has been made of welding. The spiral casing (Fig. 7), which has an inlet diameter of 3·35 m (11 ft), is built up of electrically-welded mild steel plates graduated in thickness from 32 mm (1¼ in) to 19 mm (¾ in) to suit the load, with butt joints between plate segments. The speed ring bridging the throat of the spiral casing is also electrically-welded. To facilitate transport the spiral/speed ring assembly was delivered in four complete sections, the plates of each part being welded to each other and to the speed ring quadrants in the works. At site, the sections were joined together by bolts for the speed ring and by welding for the spiral, and the finished casing was then pressure-tested to 17 atmospheres, which is 1·75 times the maximum static head. For this purpose a test cylinder was supplied for closing the throat of the casing and a test flange for closing the inlet. The spiral casing was then embedded in the foundation concrete.

The speed ring, which bridges the throat gap of the spiral casing and transmits the weight of the whole unit to the foundations, is made of cast steel in sections and has two guide rings, an upper ring to carry the generator support and turbine cover and a lower ring to carry the pivot ring. The two rings are tied together by streamlined stay vanes which guide the water to the gate apparatus.

The turbine cover which is bolted to the speed ring is fabricated of mild steel and is of box construction. It carries the swivel gate stem bearings, gunmetal bushed, and the main shaft gland. An interesting point is the sealing of this gland by sectionalised carbon rings flexibly mounted on springs and held against a steel ring on the shaft by garter springs.

The runner is made of cast steel and the vanes are protected at the outlet by stainless steel welded on the surface and then ground and polished. Labyrinth seals are provided on the runner crown and rim to reduce gap losses. The overall diameter of the wheel is 3·28 m (10 ft 9 in).

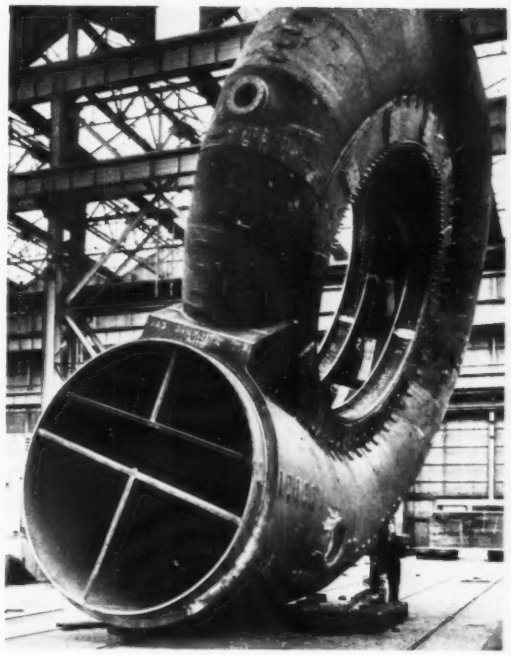

Fig. 7.—Spiral casing for 73,000 h.p. turbine, at the works

Resting on the turbine speed ring is the generator supporting barrel, which is a strong fabricated steel structure that connects the generator and turbine and transmits the generator load to the foundations. It is buried in reinforced concrete and forms the generator plinth. One of the generator support and spiral casing assemblies is shown in Fig. 8.

The draught tube is specially designed to allow removal of the runner from below. It comprises a removable throat section of the top, fitting inside the foundation ring of the turbine. Below is a cone in sections, surrounded by a gallery and having a wedge-shaped dismantling joint at the bottom. Lower still is the foundation ring of the draught tube and the steel lining of the draught tube bend, both embedded in the concrete of the foundations. To lower the runner the cone in sections is first removed along the dismantling gallery. The cap nut on the runner cover is removed and a cable attached to the main crane hook passed down the

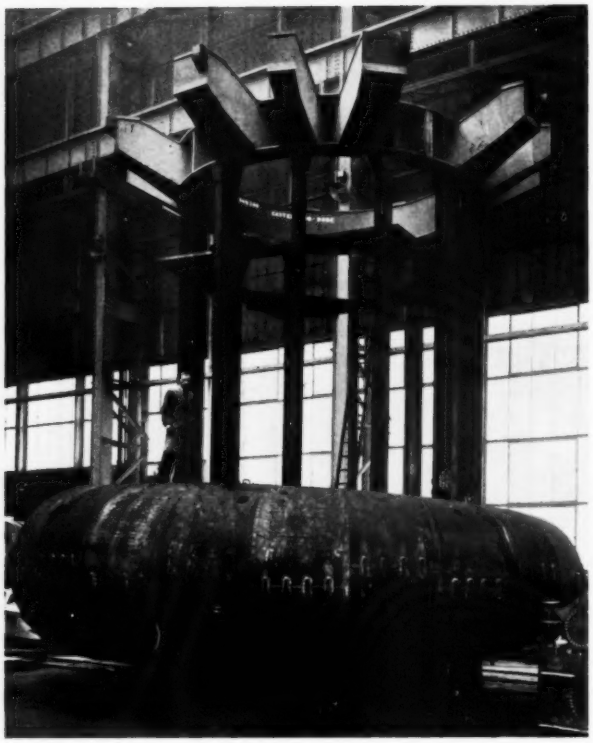

Fig. 8.—Spiral casing and generator support assembly, at the works

bore of the main shaft of the unit, whereupon the crane can be used for all the dismantling operations. Next, the draught tube throat is lowered on to a bogie (rails having been laid across the draught tube foundation ring) and taken away. Then the runner cover is removed and the runner is lowered on to the bogie. The bogie is then pulled along the dismantling gallery and the runner can be hoisted to a higher level.

The lubricating system for the turbine bearing is separate from that for the generator bearings. There are two pumps (one being a standby), each capable of supplying all the oil required. They are rated at 3 h.p. at 1,450 r.p.m. The main pump is driven by an A.C. motor and the standby by a D.C. motor fed from the station battery. If, for any reason, the oil supply from the A.C. motor fails, the D.C. motor is started automatically by means of a relay, and an alarm is sounded.

In order to prevent excessive suction on sudden drop in load and to secure smooth operation at part-gate opening, air snifting equipment is provided for admitting air to the underside of the runner. The air is admitted by the action of an automatic valve operated from the governor and is conveyed to the centre of the draught tube through radial arms and a streamlined hub.

Turbine Governing System

The governing system is automatic and oil-pressure operated. The governor actuator pendulum is driven by an electric motor which is supplied by a special alternator mounted on the main generator shaft ; it is thus operated on the synchronous electric principle. The pendulum operates a distributing valve which, by way of a pilot servomotor, controls the pressure oil to the two oil servomotors. By means of steel rods, these servomotors operate the regulating ring which opens and closes the turbine gates. The servomotors receive their pressure oil from an oil pumping unit which consists of a screw pump driven by a squirrel-cage motor of 35 h.p. at 1,450 r.p.m. Beside the pumping set is an oil pressure receiver which acts as a pressure reservoir and maintains the correct oil pressure. Air is supplied to the receiver from the station compressor. Cooling of the oil is effected by water circulating through a coil inside the oil sump.

Each turbine is provided with an emergency overspeed governing device to operate when the speed exceeds the normal by 33 per cent. A spring-loaded centrifugal pendulum is mounted on the main shaft and it closes both the turbine gates and the main inlet valves by means of a tripping gear.

' Straightflow ' Inlet Valves

The main inlet valves (Fig. 9) are of the ' Straightflow ' design, 3·35 m (11 ft) bore, and are operated by two external servomotors actuated by water pressure. The valve consists of a main body and a door, hemispherical in form, both of fabricated construction.

The door has two sections, one solid and the other pierced so as to fill the gap in the main body

and so continue the smooth bore of the main body and the pipeline when the valve is open. The solid section closes the pipe bore and has a rustless seating for a rubber sealing device which forms a water-tight joint when forced against the seating by pipeline water pressure. The valve is fitted with an isolating device to permit inspection and to enable the main water seal to be replaced if necessary without emptying the pipeline or breaking the flange joints. The valve can be operated either by remote electrical control from the turbine gauge panel or locally from the valve control panel. Fig. 10 shows a valve being lowered into position at site. These valves are believed to be the largest smooth bore rotary valves in the world.

Auxiliary Generating Sets

Underneath the loading bay and at the same level as the main machine hall are two auxiliary generating sets, each consisting of a 1,300 h.p. horizontal reaction turbine designed for an average net head of 80 m (262 ft), driving a three-phase, horizontal alternator with an output of 900 kW, 1,125 kVA at 0·8 power factor, 380 V, 50 c/s, at a speed of 1,000 r.p.m. These units are fed by their own independent pipelines, and have 'Straightflow' inlet valves of 560 mm (22 in) bore, similar in design to the valves for the main turbines. The governors are automatic, oil-pressure operated.

All the auxiliaries for the main sets are supplied by one of the two auxiliary units, one being standby to the other. Both auxiliary sets are automatically controlled for starting up and shutting down, and on failure of the low voltage supply from the set in service, it is automatically replaced by the standby set.

Main Generators

The generators are vertical shaft, enclosed, self-ventilated machines, and are arranged with two bearings, a combined thrust and guide bearing above the rotor and a second guide bearing below the rotor. The machines are rated at 45 MW, 57·4 MVA at 0·786 power factor, three-phase, 50 c/s, 15·5 kV, 214 r.p.m. The main and pilot exciters and the permanent-magnet governor generator are directly coupled to the main generator and are mounted above the rotor.

The stator frame is of welded steel and is divided into four sections for ease of shipment, each

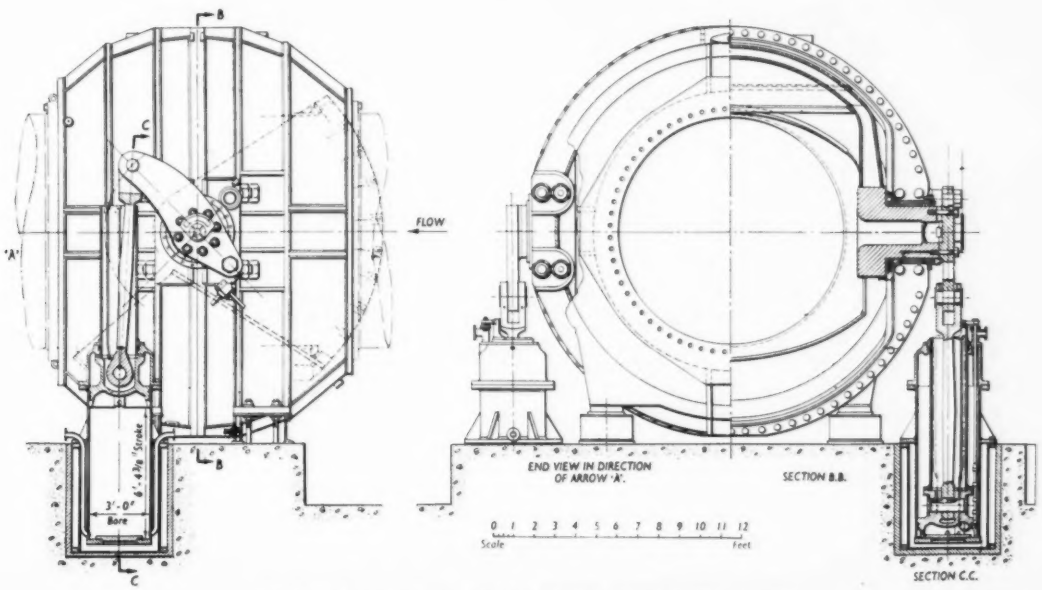

Fig. 9.—Arrangement of 11 ft bore 'Straightflow' valve

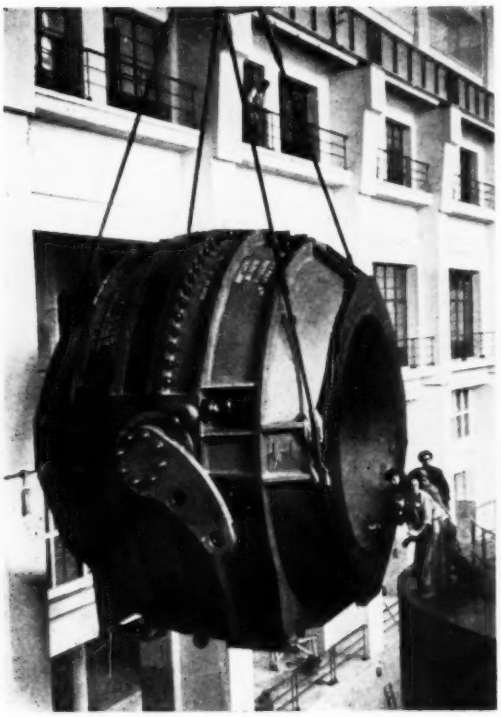

Fig. 10.—*A ' Straightflow ' valve being installed*

quarter section, weighing about 30 tons, being dispatched complete with core and windings. The four sections were bolted together at site, and the connections completed across the joints. The top of the frame has facings for the upper bracket, and the bottom is arranged for bolting direct to special facings on the steel supporting barrel already described. The core is built up of thin laminations of high-grade iron, the whole being maintained in tight compression between the endplates.

The stator has a two-layer basket winding in open slots, and all coils are interchangeable. The insulation is Class B. The coils are retained by slot wedges, and the end windings are braced against movement under short-circuit conditions. Six temperature detectors are embedded in the windings where the highest temperature is to be expected, and the leads from the elements are taken to a temperature indicating instrument.

The poles are made of laminated steel and are fitted into slots on the rotor rim and secured by taper keys. The field coils are formed of copper strip wound on edge, and damping windings are fitted in the rotor poles. The rotor body consists of a central hub keyed to the shaft and an outer rim, into which the poles are fitted. This rim is built up of laminations of high-grade ductile steel and the segments of the laminations are overlapped and secured between thick endplates. This results in a complete ring of adequate strength to withstand the stresses which occur at maximum runaway speed. Furthermore, the rim is free to expand under centrifugal force without transmitting any load to the hub due to the centrifugal effect.

The shaft is a steel forging bored throughout its length to allow the centre of the forging to be inspected, and to provide facilities for dismantling the turbine runner as already described. The complete generator rotor with shaft weighs about 240 tons and the flywheel effect is $3{\cdot}20 \times 10^6$ kg-m^2. The rotor hub and shaft can be seen in Fig. 11. The whole weight of the rotating parts plus the hydraulic thrust from the turbine is carried by a tilted-pad thrust bearing (Fig. 12). The bearing surface of a rotating thrust collar, mounted on the upper end of the generator shaft, rests on the ' babbitted ' surfaces of a number of thrust pads. Each pad is supported by a steel disc which is pivoted on a dome-shaped hardened steel insert fitted in the top of an adjusting screw. Thus, individual adjustment is possible for each pad, and each pad is free to tilt in any direction, but circumferential and radial movement is prevented by a dowel at the inner circumference and a locking plate at the outer circumference. The pad-adjusting screws are carried by a massive support ring, and, when set, are locked in position by grub screws. The support ring rests on an equaliser which provides a cushioning effect to compensate for any slight out-of-truth of the thrust face relative to the shaft axis. The equaliser rests solidly on the base of the thrust pot. A guide bearing is contained in the same thrust pot and this also consists of individually adjustable pads which bear on the vertical face of the thrust collar.

A pumped oil lubricating system is used, oil being pumped from the sump via an oil cooler to the annulus between the inner sleeve of the thrust pot and the thrust pads at the level of the bearing

Fig. 11.—*Rotor hub and shaft for* 57·4 *MVA generator*

surface. Oil is also fed to this point by natural circulation within the pot. The centrifugal pumping action of the rotating thrust face forces the oil radially outwards between the thrust pads, the correct oil level within the pot being maintained by two weirs over which the oil spills into pockets, from which it flows back to the sump. Thermometers are fitted in the bearing pads and in the oil feed to the thrust pot to sound an alarm should any abnormal condition arise. Additional thermometers in the thrust pads shut the set down at a higher temperature setting. The upper and lower guide bearings are also included in the same lubricating system which, like the turbine system, is provided with an A.C. motor-driven pump and a D.C. motor-driven pump as standby. The latter is started up automatically if the oil flow falls below a predetermined value.

A set of air-operated brakes is provided to bring the rotor to rest quickly when the set is shut down and thus avoid damage to the thrust bearing. An air compressor equipment of sufficient capacity to serve two generators is provided. The brakes are also designed to act as jacks for lifting the rotor during erection, and for this purpose high-pressure oil from an oil pump is used.

A closed circuit system of ventilation has been adopted, the air being circulated by fans on the rotor. Eight water-cooled air coolers are mounted in the annular space between the stator frame and the outer casing, and the water for these coolers is supplied from the pipeline through filters.

A complete fire quenching equipment is provided to serve three generators. Carbon dioxide gas is automatically injected into the closed ventilation system on the operation of circulating current protection or an emergency push-button switch.

The voltage of 165 kV at the secondary terminals of the transformers is kept constant over the full voltage range from no load to full load by adjusting the generator voltage by means of an automatic voltage regulator.

The sets are designed to run as synchronous condensers having an output of 40 MVA at zero power factor (over-excited). For this purpose the water level of the turbine draught tube has to be kept below the runner level at all tailrace levels, and this is achieved by admitting to the draught tube compressed air from the large air receiver and special compressor already mentioned. The general design of the combined unit, both turbine and generator, can be seen in Fig. 13.

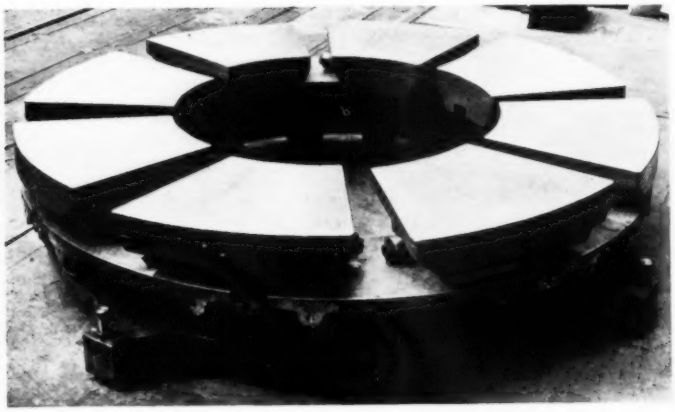

Fig. 12.—Generator thrust bearing assembly

15 kV Connections

Generation is at a nominal 15 kV. Each of the three 57·4 MVA machines is direct-connected to a 15·5/165 kV step-up transformer and switched at 165 kV. The 15 kV, 2,200 A connections are of bare copper supported on porcelain insulators, housed in chambers in the concrete on the downstream side of the station. In addition, a set of three-phase 2,200 A busbars is run in a concrete tunnel connecting these chambers. A sheet-steel link cubicle is provided in each generator-transformer circuit so that the generator can be normally connected to its associated transformer but, in emergency or during maintenance, any generator can be connected to either of the other transformers. The busbars also connect through a 15 kV oil circuit-breaker to a loading resistor capable of dissipating 50 MW for testing the generators. Interlocked control switches are provided in the link cubicles to change over secondary and indicating circuits in line with the position of the links.

Transformers

The main transformers which, as already mentioned, are installed on a platform downstream of the machine hall, are three-phase units rated at 52·5 MVA, with a voltage ratio of 15·5 kV/165 kV at full load, and 0·85 power factor. The lower voltage windings are delta connected and the high voltage side is star connected with the neutral point solidly earthed. The 165 kV windings have ±5 per cent. tappings connected to an externally-operated off-circuit tapping switch. The transformer losses are dissipated by forced oil circulation through water-cooled coolers. Each transformer weighs 120 tons (83 tons stripped for transport).

Zezere Substation

Because space is not available in the river valley for the 165 kV switchgear, the substation is mounted on top of the right-hand bank. The 165 kV overhead connections from the transformers are strung up to the roof of the power station and continue thence by stub lines, some 800 m long, to the substation. The generator breakers are at the substation and are remote-controlled from the power house control room. Surge diverters are connected to each circuit and are mounted on the power station roof as close as practicable to the transformers which they protect.

The substation (Figs. 14 and 15) contains both 165 kV and 66 kV switchgear and forms the nodal point for control of power derived from the River Zezere which, as already stated, will ultimately have three large power stations. At both voltages the switchgear is duplicate-busbar on galvanised lattice steel structures, and is of the conventional 'low-level' layout in which the busbars are supported directly from the bus-selection isolators. Busbar and feeder isolators are local-mechanically controlled. Busbar selection is off-load and the isolators are key interlocked with the breakers. Earthing contacts are provided on the outgoing side of circuit isolators.

The 165 kV equipment comprises eight bays at present, with provision for fourteen ultimately. The present circuits include those for the three generators, feeders to Lisbon and Oporto, an inter-bus transformer to the 66 kV switchgear and a bus coupler/section equipment. Extensions will cover incoming circuits from the two future power plants of the River Zezere, together with further 165 kV feeders and a second inter-bus transformer. The

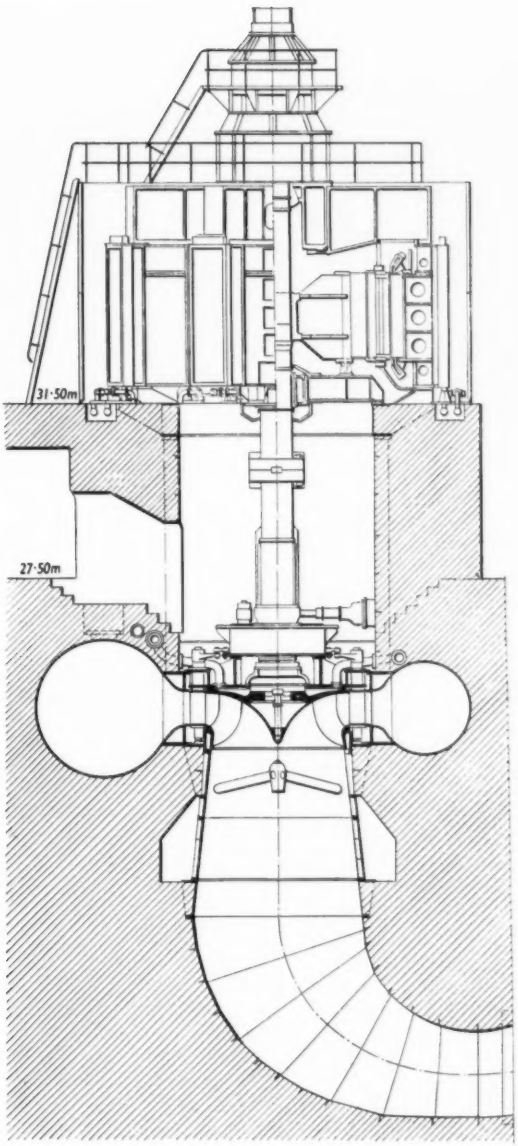

Fig. 13.—*Sectional arrangement of* 73,000 *h.p. water turbine and generator*

66 kV switchgear comprises only three bays at present (ultimately eight). This gear is to provide interconnection with existing 66 kV networks.

Surge protection is not provided on the incoming and outgoing circuits as the switchgear is no more susceptible to surges than the lines themselves. Diverters are mounted at the power station, as previously mentioned, for the protection of the generator transformers, and on each side of the inter-bus transformer.

Only the three 165 kV generator transformer circuits belong to the Hidro-Electrica do Zezere ; the contract for the remainder of the equipment was placed by the Companhia Nacional de Electricidade with the ' British Group ' and forms part of the country's transmission and distribution network.

E.H.V. Circuit-Breakers.—All E.H.V. circuit-breakers, both 165 kV and 66 kV, are air-blast equipments. At 165 kV four blast heads are used in series, the heads being mounted in pairs with a high-speed rotating sequence switch between them. The heads are shunted by non-linear resistors for voltage control and the suppression of switching overvoltages. The effectiveness of the four heads to share equally the fault duty is ensured by the symmetrical design, synchronous operation of the contacts, parallel air supplies to the blast heads, and the grading provided by the shunt resistors. The speed of operation from the receipt of a trip impulse to arc extinction is less than 3 cycles. The 66 kV breakers are similar, but use only one blast head.

The 165 kV feeder breakers are equipped for a single high-speed reclosure with ' dead time ' adjustable between 10 and 15 cycles. If a fault persists after a reclosure, the breaker re-trips and locks out. Facilities are provided for both single- and three-phase reclosure with selective control. The breaking capacity at 165 kV is 2,500 MVA and at 66 kV, 1,000 MVA, both ratings being A.S.T.A. certified. All breakers are rated for 600 A with the exception of the 165 kV coupler/section equipment which is for 800 A.

Compressor Plant.—The compressor plant for operation of the breakers is housed on the sub-station site and is designed to cater for present and future requirements at both 165 kV and 66 kV. The compressor sets, valves and pipework are all duplicated to enable any piece of apparatus to be taken down for repair or maintenance without shutting down the plant. The operation of the compressors is completely automatic, the sets being started and stopped by fall and rise of pressure in the receivers

respectively. Initial compression and storage is at 600 lb per square inch, and the air is expanded through reducing valves to half this pressure at the breaker receivers to ensure dryness.

Instrument Transformers.—At both 165 kV and 66 kV the current transformers are mounted separately from the circuit-breakers, the wound type primary being oil-immersed in a steel tank with porcelain primary bushing. Where more than one current transformer is required per phase, a common primary is used with multiple cores and secondaries.

Auxiliary Switchgear

Because of the importance of power station auxiliary supply, it is duplicated and made independent of any source external to the station. Two hydro-electric sets are installed, each of which is capable of supplying the total requirements of the station.

Generation is at 380 V, three-phase, three-wire, and power is fed to a single-bus main auxiliaries board with a section breaker between the generator circuits. Normally this board is run with one generator only in service and the bus-section closed. If, for any reason, the running generator trips out, then the standby machine is started automatically and switched in, this sequence being initiated by an undervoltage relay on the bars. The main sets can run for approximately ten minutes without auxiliary supply, while the starting and switching of the standby auxiliary plant is accomplished within three minutes.

The two generator circuits and the bus-section are controlled by 2,400 A air-break circuit-breakers, remotely operated from the control room. The heavier circuits from the switchboard are also controlled by air-break circuit-breakers, but they are of 600 A rating and manually operated. Smaller circuits are fed from metal-enclosed fuse-switch units. The main auxiliaries board supplies the power station, the dam, the settlement and the substation.

In addition, each main generator-transformer set is provided with its own essential auxiliaries board, comprising fuse-switch units and latched-in contactors for the circuits associated exclusively with it. Each essential auxiliaries board is fed by duplicate cables, one from each section of the main auxiliaries board. Certain vital services, such

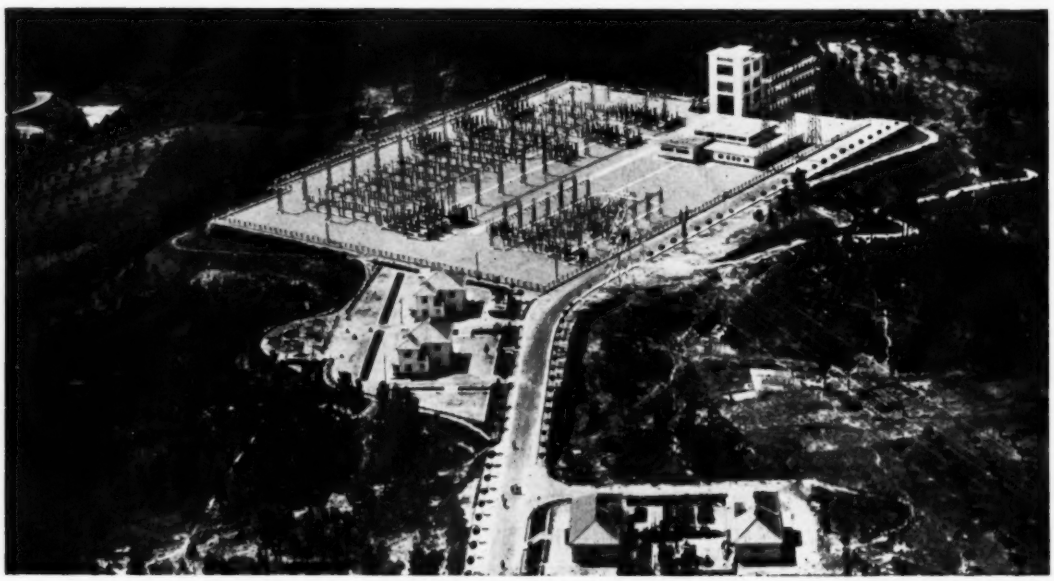

Fig. 14.—*Zezere substation from the air*

as lubricating pumps, are provided with emergency D.C. pumping sets which are automatically switched on to the battery on failure of A.C. supply. The starting here is initiated by cessation of oil flow, etc. ; it is therefore independent of electrical functions.

At the substation the auxiliary supply is taken from an 11 kV tertiary winding on the 165/66 kV inter-bus transformer, and then stepped down to 380 V by a 250 kVA station transformer. A stand-by supply is provided from the power station main auxiliaries board. All lighting supplies are taken from the auxiliary boards through three-wire/four-wire lighting transformers to reduce the fault capacity on the lighting circuits and also to avoid the necessity of making the auxiliary boards four-wire throughout.

Controls

Independent controls are provided at the power station and the substation because, as already stated, the equipments belong to different authorities. The H.E.Z. controls the output from the generators and the C.N.E. the distribution at 165 kV and 66 kV.

The power house control room overlooks the machine hall. The control board is of the conventional vertical sheet steel cubicle form, arranged around three sides of a rectangle, with a desk board in the centre. It is equipped with a full mimic diagram, instruments, controls and alarms for the three main generator-transformer sets, including their associated 165 kV breakers at the substation, and for the two auxiliary generators and the bus-section breaker on the auxiliary board. Also controlled from here is the 15 kV circuit-breaker for the loading resistance. The equipment includes automatic voltage regulators, synchronising gear, and master frequency indication. A hydraulic control cubicle provides remote control and indication from the dam. Relays and metering are mounted on cubicles housed in separate rooms adjacent to the control room.

At the substation the controls are housed in a building in the switchyard. The control board is of the same general form as that at the power house, being of vertical sheet steel panels, without the desk, and is arranged on four sides of a square. It provides control for all 165 kV and 66 kV

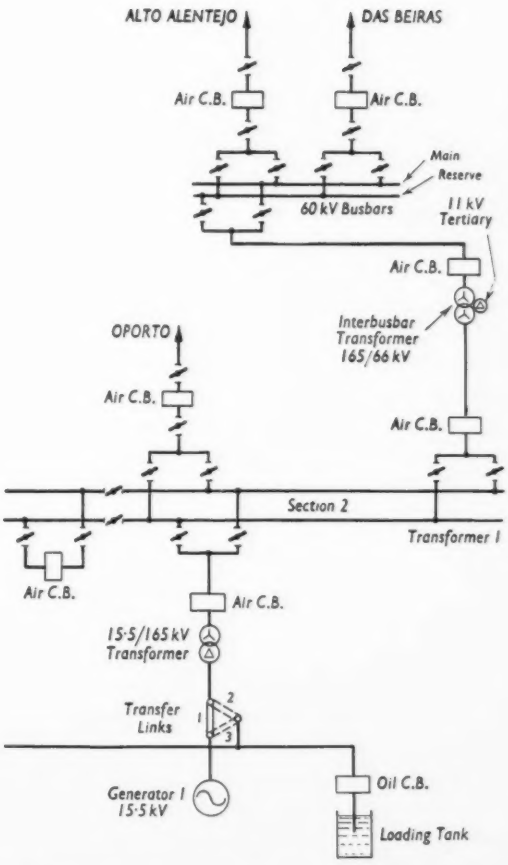

Fig. 15.—Key diagram of Zezere substation, omitting the circuits for generators Nos. 2 and 3

feeders, the inter-bus transformer and the coupler-section equipment. Check synchronising is fitted to all feeder circuits. Relays and meters are again housed separately from the controls.

Protection

The generator neutrals are each earthed through a voltage transformer shunted by a non-linear resistor. The 165 kV and 66 kV star points of the transformers are earthed solidly.

The main generators are provided with circulating current protection, together with overcurrent back-up, the latter operated from current transformers in the star point. Overvoltage protection

is also provided. Generator earth-fault is limited to the current which can be passed by the neutral voltage transformer. The generator can therefore continue to operate with an earth-fault on one phase, but a relay connected to the voltage transformer gives an alarm that such a condition exists. A rotor earth-fault also gives an alarm. Balanced voltage protection covers the main transformers, and includes the stub-lines to the substation in the protective zones. The main transformers are fitted with Buchholz relays, and oil and winding temperature indicators and alarms.

The auxiliary generators are protected by circulating current backed up by overcurrent and earth-fault protection, together with overvoltage relays. The inter-bus transformer is protected by balanced voltage, together with Buchholz and back-up overcurrent and earth-fault protection on both sides.

The 66 kV feeders are fitted with directional protection. For the 165 kV feeders, back-up protection only has been provided by the 'British Group.' The line protective relays were the subject of a separate contract placed by the Companhia Nacional de Electricidade, which is intended to apply to the whole of the Portuguese E.H.V. network. These protective relays, however, in the case of the Zezere substation, were mounted and wired on panels provided as part of the main switchgear contract.

General Station Equipment

Power House Crane.—In the power house there is an electric overhead travelling crane designed to handle a maximum working load of 260 tons (the heaviest lift is the generator rotor with a weight of about 240 tons) and having motions of main hoisting (two speeds), auxiliary hoisting (20 tons), traversing and travelling. It is operated by four electric motors designed for 380 V, three-phase, 50 c/s.

The main hoist controller consists of an enclosed contactor panel operated by a drum master controller with crank handle. The other controllers are upright air-break drum controllers with crank handles. All controllers have 'off' position interlocks, and the hoist controllers are suitable for working in conjunction with shunt limit switches to prevent overwinding. Automatic electric brakes are provided ; they are operated by a 'thrustor' connected in such a way that the brake is released immediately the motor is started and is applied immediately the current is cut off or fails for any reason.

Disperser Valves.—Two disperser valves are installed for operation on the two 3 m (9 ft 10 in) diameter scour culverts, one of which is on each side of the power station. Each valve discharges 150 cubic metres (150 tons) of water per second under a maximum head of 95 m (312 ft). The energy is effectively dispersed by converting the solid jet into a hollow cone, to avoid erosion of the banks of the narrow gorge and the river bed.

Draught Tube Gates.—A set of draught tube gates is provided for the main turbines, comprising two gates of steel construction 6·4 m (20 ft 11 in) wide by 3·35 m (11 ft) high with rubber seals and gun-metal guide strips and a by-pass valve located in one gate only. One draught tube gate is also provided for the auxiliary turbines ; it is made of timber, 1·53 m (5 ft) wide by 1·53 m (5 ft) high. For handling the parts of the disperser valves and the draught tube gates, an electric jib travelling crane, capable of lifting 25 tons, is provided. The motions of hoisting, slewing and travelling are each operated by an independent motor.

Drainage and Dewatering Pumps.—Two drainage pumps are provided for draining the station pits, each consisting of a vertical centrifugal pump driven by a 12 h.p. electric motor. For dewatering the draught tubes there are two pumping sets, each comprising a vertical pump with a 60 h.p. motor.

Flow Meters.—Three aerofoil flow meters are fitted in the pipes leading to the main turbine valves, each comprising an aerofoil wing of bronze with rustless ball bearings and a set of transmitting flow indicating and recording instruments.

Ancillaries.—Ancillary equipment includes batteries and charging gear at both power house and substation, and also an automatic telephone exchange.

Other items of general equipment are purifying equipments for turbine and generator oil and for transformer oil, and a testing equipment for transformer oil.

Manufacturers of the Plant and Equipment

The manufacturers of the main items of plant and equipment in the Castelo do Bode power station and Zezere substation, as described in this article, were as follows :—

Main and auxiliary water turbines and inlet valves, main and auxiliary generators, The English Electric Company, Ltd. ; main transformers, Metropolitan-Vickers Electrical Company, Ltd. ; power station and substation switchgear, Metropolitan-Vickers Electrical Company, Ltd. ; disperser valves for scour culverts, The English Electric Company, Ltd. ; power station crane and jib crane, Sir William Arrol and Co., Ltd. ; draught tube gates, Sir William Arrol and Co., Ltd. ; purifying equipment for turbine and generator oil, Alfa-Laval Company, Ltd. ; purifying equipment for transformer oil, Streamline Filters, Ltd. ; main and control cables, British Insulated Callender's Cables, Ltd. ; overhead line to substation, British Insulated Callender's Construction Company, Ltd.

This article will be concluded in Part Two, to be published in the September 1954 *issue of this journal* (*Volume* 13, *No.* 7), *with a description of the River Cavado Power Scheme.*

The Napier Differential Pressure Gauges

IN THE development of turbine engines and fluid control systems, it is frequently necessary to measure, to a high degree of accuracy, the difference between two pressures where the magnitude of the differential is relatively small in comparison with the actual pressure level being measured.

Measurement of the two pressures by independent gauges and subtraction of their readings is inherently inaccurate. For example, where a differential of 50 p.s.i. is required to be measured at a pressure level of 500 p.s.i., an error of $+1\%$ and -1% respectively in the measurement of each of two pressures of 500 p.s.i. and 450 p.s.i. will amount to approximately 10 p.s.i. in the resultant differential, thus giving an intolerably high error of 20%. It is therefore necessary that the measurement should be performed by a single measuring element such as a capsule or Bourdon tube housed in a case which will safely withstand the high pressures involved and permit observation of the dial without hazard to an operator.

With the exception of a restricted range of aircraft flight test instruments, there is no commercial instrument of this type available. In order to meet the requirements of current research programmes, the Luton Flight Development Establishment of D. Napier and Son Limited has designed and developed a series of high pressure differential gauges in two principal sizes for use in ground and airborne installations respectively.

A differential pressure gauge suitable for ground installations where hydraulic pressures are involved is shown in the sectional drawing, Fig. 1. This type is produced in a series covering differential pressure ranges of 0 to 50, 0 to 100, 0 to 150 and 0 to 200 p.s.i., and is designed to operate at a maximum working pressure level of 1,100 p.s.i.

The high pressure casing of this instrument is manufactured of light alloy, the cylindrical body of which has an internal shelf to support the 'Armourplate' glass observation window. Pressure sealing of the window is provided by an 'O' ring housed in a recess in the shelf, and the glass is also packed around its circumference to prevent contact with the metal body. The window is secured by an external retaining plate with a packing washer again preventing metal contact with the glass. At the rear of the case a detachable back plate is secured to the body by studs, and a pressure-tight joint is provided by a sealing ring retained in a recess in the body.

The pressure gauge movement, consisting of a standard Bourdon tube mechanism fitted with a graduated dial and pointer, is attached to the back plate by three small studs. The pressure connection of the movement, passing through a hole at the base of the back plate, is fitted with gaskets and an external adaptor to provide pressure-tight seals, the pressure connection to the case being supplied by a screwed fitting secured directly to the rear face of the back plate.

Situated at the top of the cylindrical body is a small air vent screw to enable the case to be completely filled with liquid. Due to the considerable mass of the instrument, tapping before taking a reading requires to be somewhat heavier than can be done with the finger tip or a pencil and, to facilitate this, one of the window retaining plate nuts is made in the form of an anvil which can be tapped with a spanner or other convenient article. Around the front face of the casing is a large attachment flange provided with four holes to enable the gauge to be installed in a test panel.

As all materials used in the construction of this gauge are non-corrodible, and all aluminium alloy parts anodised, it may be used with a variety of liquids as the hydraulic medium. Each assembled case, complete with observation window, is proof tested at 2,200 p.s.i., after which the pressure gauge movement is fitted and the completed instrument again pressure tested at 1,250 p.s.i. An accuracy

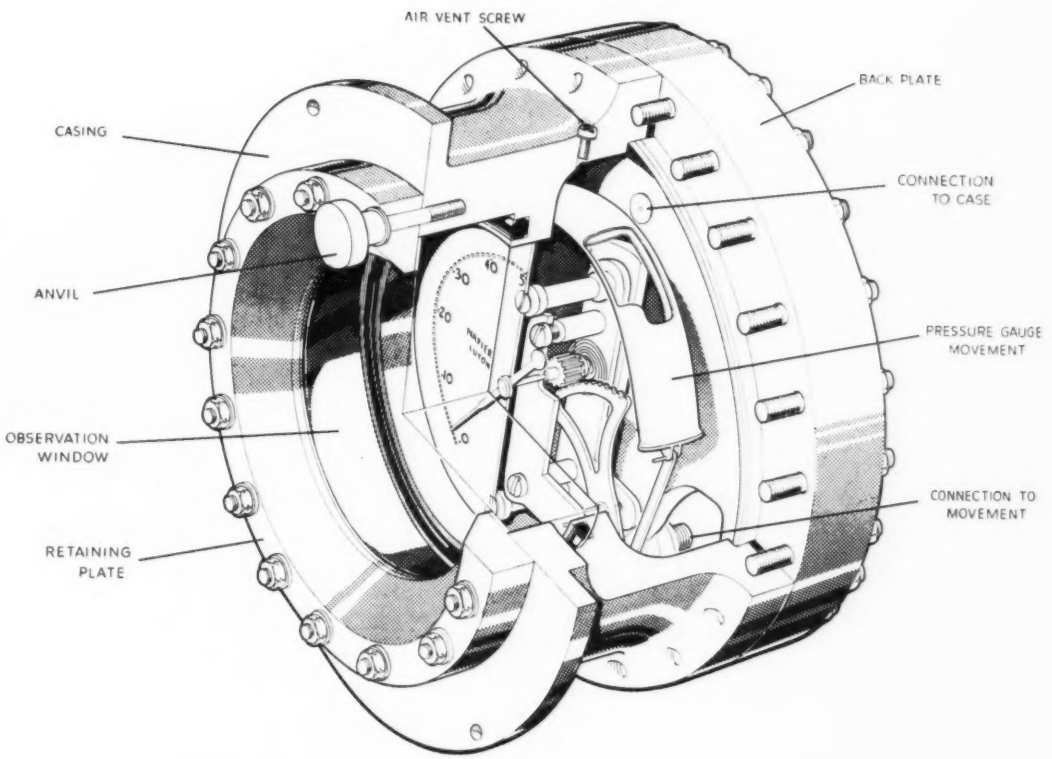

Fig. 1—Differential pressure gauge for ground installation. Maximum working pressure level 1,100 *p.s.i.*

of measurement of $\frac{1}{4}\%$ of full-scale indication is obtainable by employing a Budenberg standard test gauge movement.

A second type of pressure gauge, specifically designed for airborne installations and illustrated in Fig. 2, has been developed for the measurement of supercharger boost pressure relative to zero absolute pressure, with an operating range of 0 to 100 p.s.i. In accordance with common practice, the Bourdon tube of the movement fitted to this instrument is evacuated, and the pressure to be measured is connected to the inside of the casing. When recording high gaseous pressures, it is considered that the hazard to flight crews in the event of failure of a toughened glass window is not justified, however remote this possibility may be, and therefore an arrangement employing a magnetic transmission to the instrument pointer is adopted.

The pressure gauge movement is housed in a light alloy casing and supported on three tubular pillars from a mounting plate, which in turn is secured to the rear of the casing by an integral adaptor. This mounting is designed to ensure that the instrument mechanism is unaffected by any distention of the case due to the applied pressure. The adaptor provides the pressure connection to the case, a pressure-tight seal being made by an internal gasket and an external clamp nut. Replacing the normal pointer is a small rectangular magnet mounted directly on to the original pointer spindle of the movement.

The detachable face of the instrument consists of a heavy brass dial plate with a central diaphragm of beryllium copper and contains an independent pointer, a graduated dial, and a glass window retained by a circlip. The pointer spindle

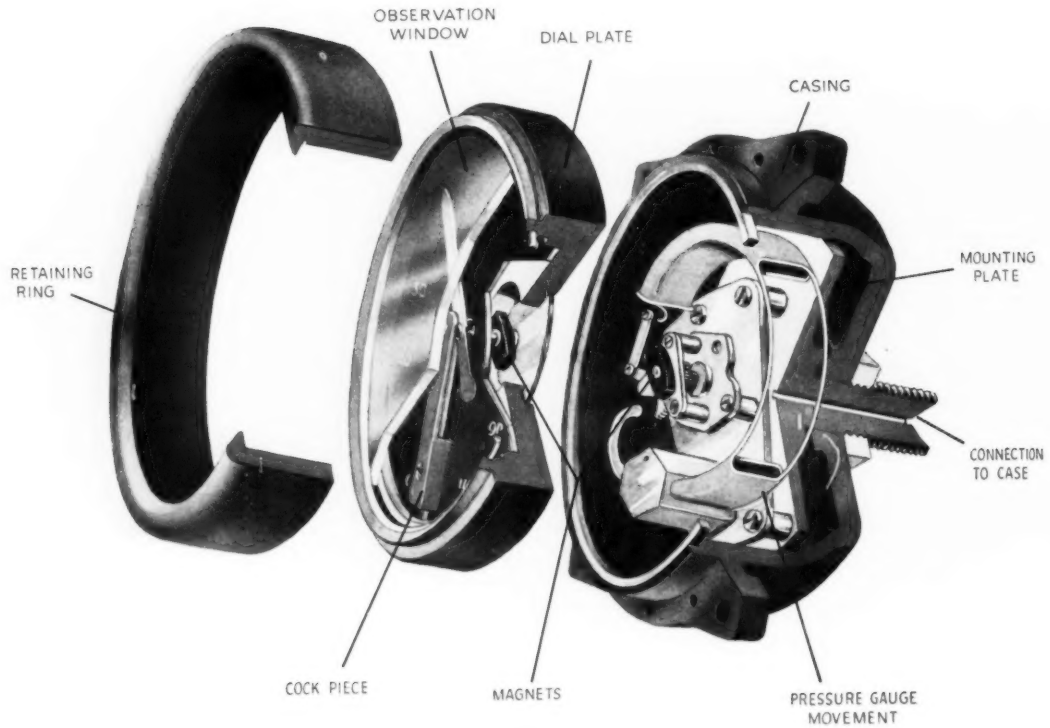

Fig. 2—Supercharger boost pressure gauge for airborne installation

is supported between two jewelled bearings, the rear bearing being a combined thrust and journal type retained in a housing on the front face of the dial plate assembly. Situated in front of the dial is a radial cock-piece which carries the front journal bearing. A second magnet, similar to that fitted to the pressure gauge movement, is mounted on the pointer spindle behind the dial, and therefore transmits any rotation of the mechanism to the pointer itself.

The complete dial assembly is secured to the instrument case by a retaining ring and twelve screws, a pressure tight seal being made by a sealing ring housed in a recess on the front face of the casing. Four lugs are provided on the case for attachment to an instrument panel.

A number of variations of this gauge have been developed for the measurement of differential gaseous pressures in airborne and ground installations. Some instruments are fitted with capsules and cover differential pressure ranges of −4 to +4 p.s.i., and 0 to 1 in stages up to 0 to 15 p.s.i., whilst others are fitted with Bourdon tube mechanisms to cover a maximum range of 0 to 45 p.s.i. These instruments have independent pressure connections to both the movement and case, and the entire series is suitable for operating at a pressure level of 100 p.s.i.

Increasing use of electronic recording from variable impedance or strain-gauge pressure transducers may in many instances displace instruments of the dial and pointer type, but for airborne work where visual observation is essential, and for the majority of work on development test rigs, the conventional dial instrument cannot be dispensed with. Both types of pressure gauge described were designed for particular applications, but they have proved extremely valuable over a long period of development work, having been employed on a great variety of projects.

The Flow of Power and Reactive Components in Rectifier and Inverter Equipments

By T. E. CALVERLEY, B.Sc., A.M.I.E.E., Chief Engineer, Rectifier Department.

PART TWO

Part One of this article was published in the March 1954 issue of this Journal, Volume 13, No. 5.

II.—MODIFICATION TO SIMPLE THEORY TO ALLOW FOR FINITE A.C. REACTANCE

In making allowance for finite A.C. reactance the first step is taken towards practical operating conditions. The calculations in this section will show how the secondary current is altered in wave shape due to A.C. reactance, thereby altering the constituent components in magnitude and phase but not eliminating or introducing any components. Since, with balanced conditions, each secondary current will be altered the same amount, it follows that the corresponding components in each secondary circuit will suffer the same alteration in magnitude and phase. Therefore, the principles of 'transmission' and 'cancellation' may be still applied but each component must be corrected from its value derived in Section I.

Assumptions

The assumptions made in this section are :—

(*a*) Zero grid delay.

(*b*) Infinite inductance of D.C. load.

(*c*) Zero rectifier arc drop.

(*d*) Zero transformer and circuit resistance.

(*e*) Zero transformer magnetising current.

An allowance for (*c*) and (*d*) is made at the end of this section.

Analysis of Secondary Current Wave-form

The presence of A.C. reactance introduces a finite time during which commutation occurs between secondary phases, thereby causing the vertical rise of secondary current shown in Fig. 6 to be modified to that shown as i_1 in Fig. 12b. Also during this period of commutation, called the angle of overlap μ_o, the D.C. voltage wave-form is modified as in Fig. 12a. The block of secondary current is modified to contain three functions which can be shown to be represented by the following equations :—

$$i_1 = I_s (1 - \cos\theta) \text{ from } 0 \text{ to } \mu_o \quad . \quad . \quad . \quad . \quad (19)$$

$$i_2 = I_d \qquad \text{from } \mu_o \text{ to } \frac{2\pi}{p} \quad . \quad . \quad . \quad . \quad (20)$$

$$i_3 = I_d - I_s \left\{ 1 - \cos\left(\theta - \frac{2\pi}{p} \right) \right\} \text{ from } \frac{2\pi}{p} \text{ to } \frac{2\pi}{p} + \mu_o \quad . \quad . \quad . \quad . \quad (21)$$

where I_s is the peak current flowing if two commutating secondary windings are short-circuited, and is calculated by

$$I_s = \frac{I_d}{1 - \cos\mu_o} \quad . \quad . \quad . \quad . \quad . \quad . \quad . \quad (22)$$

Fourier analysis of the secondary current made up of these three functions gives the following result :—

(a) D.C. component $I_{ms\mu} = \frac{I_d}{p}$ . . . . . (23)

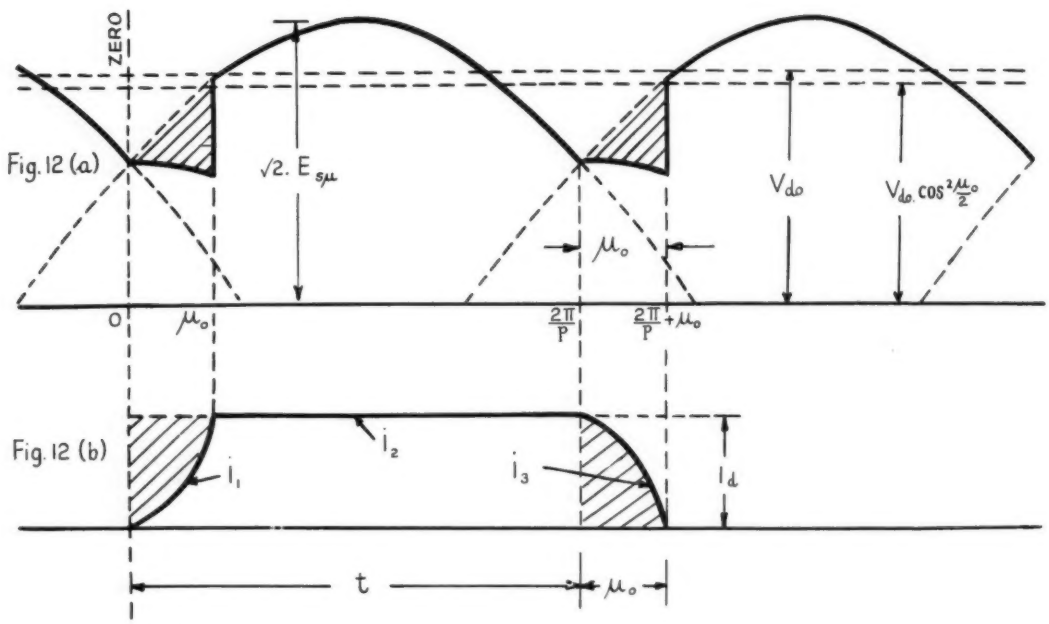

Fig. 12.—Modification due to A.C. reactance of (a) D.C. voltage wave-form, (b) secondary current

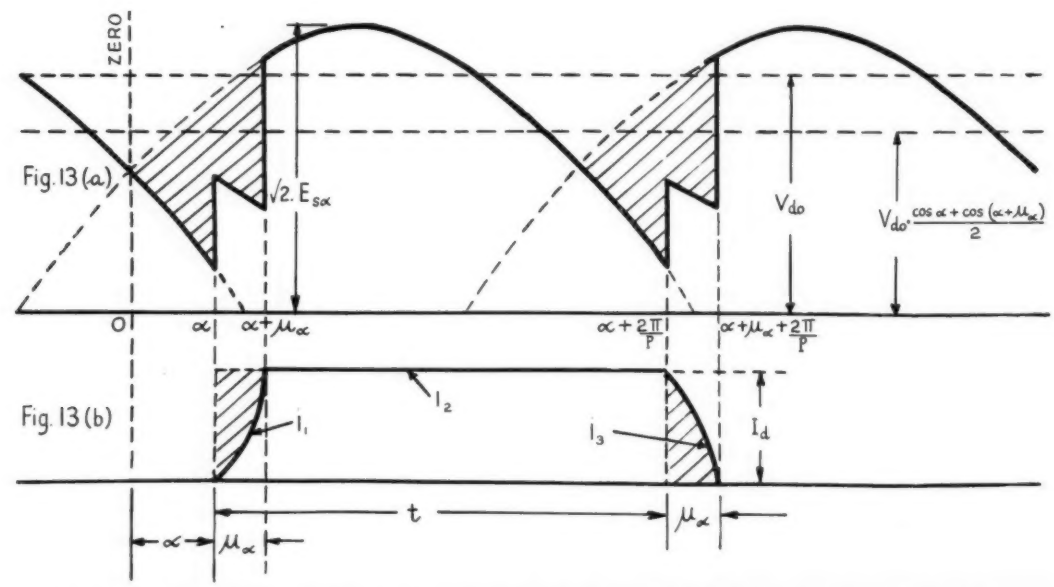

Fig. 13.—Modification due to A.C. reactance and grid control of (a) D.C. voltage wave-form, (b) secondary current

(b) R.M.S. value of *nth* harmonic

$$I_{ns\mu} = \frac{I_d}{n\pi} \cdot \sqrt{2} \cdot \sin \frac{n\pi}{p} \cdot \omega(n\mu) \quad . \quad . \quad . \quad (24)$$

where $\omega(n\mu) = \sqrt{\{n^2 \sin^2 \mu_o + \cos^2 \mu_o + 1 - \ldots 2(n . \sin n\mu_o . \sin \mu_o + \cos n\mu_o . \cos \mu_o)\}}$

$$(n^2 - 1)(1 - \cos \mu_o)$$

Since this article is concerned mainly with flow of power, expressions for the phase positions of the harmonics will not be quoted. Equation 24 has in fact been quoted here only to illustrate that the approach made in the previous section, i.e. equating 'n' to unity in the harmonic equation, no longer holds, since with 'n' equal to unity in equation 24 the solution becomes indeterminate. A new approach can be made by assuming that the power transmitted by all the secondary phases is equal to the power output.

Simple theory again shows that the output D.C. voltage, corrected for the effect of overlap, is given by

$$V_{d\mu} = V_{do} . \cos^2 \frac{\mu_o}{2} \quad . \quad . \quad . \quad . \quad . \quad . \quad (25)$$

where V_{do} is given by equation 18.

The D.C. power output is $V_{d\mu} . I_{dc}$, and equating this to the total secondary circuit power it can be shown that the R.M.S. value of the fundamental frequency component *in phase* with the secondary voltage is given by

$$I_{1s\mu p} = \frac{I_d}{\pi} \sqrt{2} . \sin \frac{\pi}{p} . \cos^2 \frac{\mu_o}{2} \quad . \quad . \quad . \quad . \quad (26)$$

To obtain the *quadrature* or reactive component it is necessary to evaluate the reactive power in a secondary phase :—

$$P_{1s\mu r} = \frac{p}{2\pi} \int e.i.d\theta \quad . \quad . \quad . \quad . \quad . \quad (27)$$

where i = instantaneous current
and e = instantaneous value of quadrature component of voltage.

The reactive component of secondary current derived from equation 27 is

$$I_{1s\mu r} = \frac{I_d}{\pi} \sqrt{2} \sin \frac{\pi}{p} . \left\{ \frac{2\mu_o - \sin 2\mu_o}{4(1 - \cos \mu_o)} \right\} \quad (28)$$

Examination of equations 26 and 28 shows that they contain the common factor $I_d . \frac{\sqrt{2}}{\pi} . \sin \frac{\pi}{p}$ which is in fact the fundamental component with zero A.C. reactance, i.e. I_{1so} as given by equation 4. Hence, two correction factors for the fundamental component of secondary current, as discussed in the Introduction (Method of Approach), may be quoted.

Power component correction factor

$$\omega(1\mu)p = \cos^2 \frac{\mu_o}{2} \quad . \quad . \quad . \quad . \quad . \quad . \quad . \quad (29)$$

Reactive component correction factor

$$\omega(1\mu)r = \frac{2\mu_o - \sin 2\mu_o}{4(1 - \cos \mu_o)} \quad . \quad . \quad . \quad . \quad (30)$$

As would be expected, the introduction of A.C. reactance is linked with the requirements of reactive current or kVA. The value of the reactive and power component may be calculated by selecting the appropriate current from column n equal to 1 in Table II, III or IV and applying the correction factors given in equations 29 and 30.

Significance of Secondary Current Wave-form Analysis

The components of secondary current calculated under the previous heading can be applied to the equivalent circuit diagram, as was done in Section I.

D.C. Component

For the same direct-current output the D.C. component must retain the same value as in Section I.

A.C. Components of Fundamental Frequency

Consider an ideal rectifier equipment with an infinitely inductive load and in which variable reactance may be placed in the A.C. side as required. With no A.C. reactance and a secondary voltage of $E_{s\mu}$ the D.C. voltage can be calculated

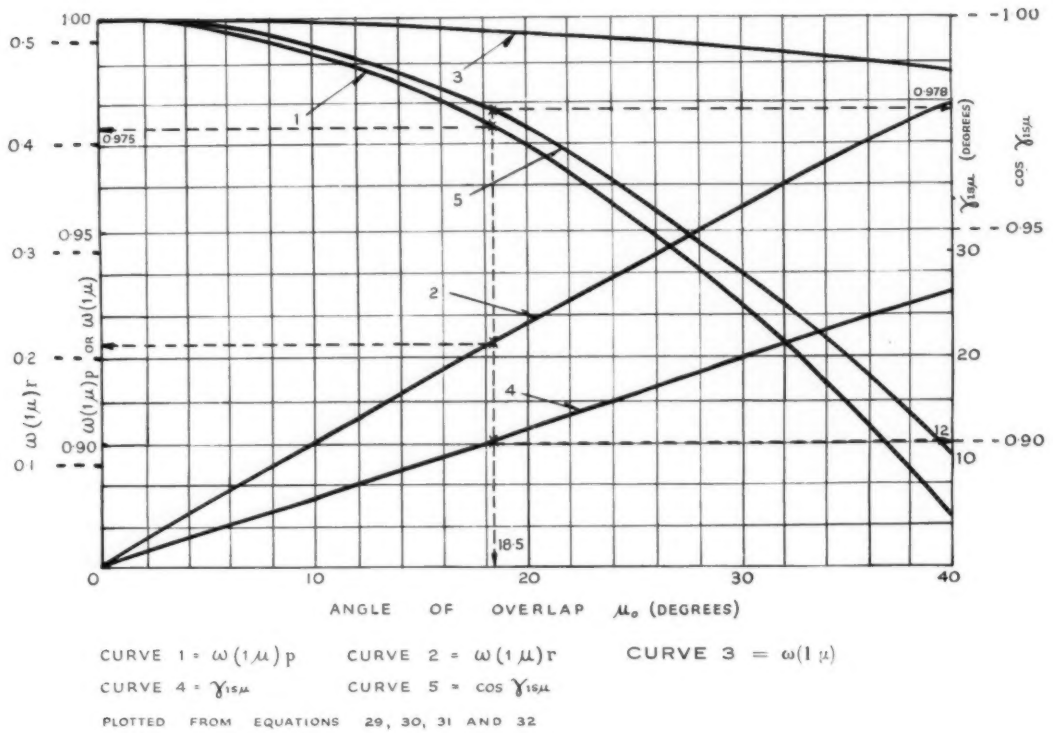

Fig. 14.—*Influence of overlap on fundamental component of secondary current*

from equation 18 and the various current components from Tables II, III and IV for a given direct current I_{dc}. Now let the A.C. reactance be increased progressively causing an increase in the angle of overlap, while maintaining the direct current constant. The power component and reactive component of secondary current will have to vary according to equations 26 and 28. The correction factors to obtain these quantities are plotted in Fig. 14, from which it can be seen that the power component will decrease but the reactive component will increase from zero. This in effect means that the R.M.S. fundamental component is suffering a phase displacement or in other words, the power factor is departing from unity. Curve 4 of Fig. 14 shows how the angle of displacement varies with the angle of overlap, and curve 5 is the cosine of this angle, *i.e.* the power factor.

The process of secondary current analysis thereby gives a means of calculating power factor without any reference to the primary side of the equipment.

To complete the calculations relating to the fundamental component it can be shown from the equations already derived that the R.M.S. fundamental component of secondary current is given by

$$I_{1s\mu} = \frac{I_d \sqrt{2}}{\pi} \cdot \sin\frac{\pi}{p} \cdot \frac{\sqrt{\{(1-\cos 2\mu_o)^2 + (2\mu_o - \sin 2\mu_o)^2\}}}{4(1-\cos\mu_o)} \quad (31)$$

and that the tangent of the angle of displacement is given by

$$Tan\ \gamma_{1s\mu} = \frac{2\mu_o - \sin 2\mu_o}{1-\cos\mu_o} \quad . \quad . \quad . \quad . \quad (32)$$

In Fig. 14 the various correction factors for the fundamental component of current are plotted for easy reference.

Allowance for Copper Loss and Arc Loss

Copper loss in the transformer and arc loss in the rectifier will be designated by P_{cu} and P_{arc} respectively. The increment of D.C. voltage to overcome this loss may be obtained from

$$\Delta V_{dc} = \frac{P_{cu} + P_{arc}}{I_{dc}} \quad . \quad . \quad . \quad . \quad . \quad (33)$$

Practical Example

The example chosen in Section I will be used again, only in this case it will be assumed that in

TABLE VII

EXAMPLE OF POWER BALANCE

$p = 3 \quad m = 4 \quad k = 4$

Quantity	Equation	Reference	Example
D.C. power output	$P_{d\mu} = V_{d\mu}.I_{dc}$	—	5,000 kW
D.C. voltage	$V_{d\mu}$	—	500 volts
Direct current	I_{dc}	—	10,000 amp
Angle of overlap	μ_o	Simple theory	18·5°
Increment of D.C. voltage for losses	$\Delta V_{dc} = \frac{P_{cu}+P_{arc}}{I_{dc}}$	*Eqn.* 33	28 volts
Total rectifier e.m.f.	$V_{do} = \frac{V_{d\mu}+\Delta V_{dc}}{\cos^2 \frac{\mu_o}{2}}$	*Eqn.* 25	541 volts
Secondary voltage	$E_{s\mu} = \frac{V_{do}\pi}{\sqrt{2}.p.\sin\frac{\pi}{p}}$	*Eqn.* 18	462 volts
R.M.S. fundamental component of secondary current ($\mu_o = 0$).	$I_{1so} = \frac{I_d\sqrt{2}}{\pi}.\sin\frac{\pi}{p}$	*Eqn.* 4	975 amp
R.M.S. fundamental component of secondary current (power component, $\mu_o = 18{\cdot}5°$)	$I_{1s\mu p} = I_{1so}.\omega(1\mu)p$	Fig. 14	950 amp
R.M.S. fundamental component of secondary current (reactive component, $\mu_o = 18{\cdot}5°$)	$I_{1s\mu r} = I_{1so}.\omega(1\mu)r$	Fig. 14	204 amp
Power factor	$\cos \gamma_{1s\mu}$	Fig. 14	0·978
Total secondary power	$P_{s\mu} = m.p.I_{1s\mu p}.E_{s\mu}$	—	5,275 kW
R.M.S. fundamental component of primary current (power component).	$I_{1p\mu p} = I_{1s\mu p}.\frac{E_{s\mu}}{E_p}.K$	—	158 amp
Total primary power	$P_{p\mu} = 3.E_p.I_{1p\mu p}$	—	5,275 kW
R.M.S. fundamental component of line current (power component).	$I_{l p\mu p} = \sqrt{3}\,.\,I_{1p\mu p}$	—	275 amp
Total line power	$P_{l\mu} = 3.I_{l p\mu p}.\frac{E_p}{\sqrt{3}}$	—	5,275 kW

the design of the equipment allowance has to be made for A.C. reactance, copper loss and arc loss. A table of power flow will be drawn up again as in the previous example, using the equations derived on the basis of Fourier analysis of the secondary current.

Equipment particulars are :—

D.C. power output	$P_{d\mu}$	..	= 5,000 kW.
D.C. voltage	$V_{d\mu}$	..	= 500 volts.
Direct current	I_{dc}	..	= 10,000 amp.
Connection T in Table IV			= quadruple zig-zag with delta primary.
A.C. primary voltage	E_p	..	= 11,000 volts.
% reactance referred to primary kVA	$\% X_c$		= 10%.
Copper loss	P_{cu}	..	= 75 kW.
Arc loss	P_{arc}	..	= 200 kW.

Table VII shows the calculation of the power balance. The angle of overlap μ_o is calculated by simple theory given in the text books. The required value of V_{do} is calculated, allowing for reactance drop and losses to give the terminal voltage of 500 volts, and thence the secondary voltage $E_{s\mu}$ is derived. This settles the turns ratio of the transformer. By means of the correction factors plotted in Fig. 14 the power component of secondary current is derived and the power factor determined, thus enabling the power in each part of the circuit to be calculated. Although the power output is 5,000 kW, that in the other part of the circuit is 5,275 kW due to the arc and copper losses. In actual practice this is not strictly true as part of the copper loss occurs in the primary, but to consider all loss in the secondary circuit is sufficiently accurate to illustrate the mathematical theory.

It is of interest to note that the power factor can be read off directly from Fig. 14 (as it is only a function of the overlap angle μ_o), but it must be remembered that a rectifier can have its power factor quoted in two distinct ways. The value obtained from Fig. 14 is that normally called the 'Displacement Factor' and is the quantity required by B.S. 1698 : 1950, *i.e.* it is the '$\cos \phi$' of the fundamental component of supply current. The power factor derived from the ratio of kW to kVA would have a lower value since the kVA quantity contains harmonic components as well as the fundamental component.

The power and reactive components of the fundamental line current can be calculated directly from Tables II, III and IV and corrected by the factors in Fig. 14. Using the example of Table VII to illustrate the procedure, the value of $I_d \cdot E_{s\mu}/E_p = 2{,}500 \times 462/11{,}000 = 105$ amp. From Table IV, connection *T*, the line current is 270% of this for no overlap, *i.e.* 283 amp. Now, from Fig. 14 for μ_o equal to 18.5°, the power component correction factor is 0.975 and the reactive component correction factor is 0.210. This gives the corrected power component in the line as $283 \times 0.975 = 275$ amp, and the corrected reactive component in the line as $283 \times 0.210 = 59.5$ amp.

III. MODIFICATIONS TO SIMPLE THEORY TO ALLOW FOR A FINITE A.C. REACTANCE AND GRID CONTROL

In the previous sections equations have been derived for the current in different parts of the rectifier circuit and modified to allow for practical conditions of finite A.C. reactance, arc drop and losses. It is now proposed to carry this a stage further and introduce grid control. As in Section II, equations will be stated which determine the secondary current wave shape and this will be analysed by Fourier analysis ; since it will be assumed that all secondary phases are equally grid-delayed, the principle of 'transmission and cancellation' can again be applied. A series of correction factors will be obtained in order to correct the equations derived under the 'Simple Rectifier Theory' (Section I) to allow for grid control and A.C. reactance.

Assumptions

The assumptions made in this section are :—

(*a*) Infinite inductance of D.C. load.

(*b*) Zero rectifier arc drop.

(*c*) Zero transformer and circuit resistance.

(*d*) Zero transformer magnetising current.

An allowance for (*b*), (*c*) and (*d*) is made at the end of this section.

Analysis of Secondary Current Wave-form

The effect of grid control is to delay the instant of firing of each anode by an angle called the

'delay angle', and consequently to reduce the mean D.C. voltage. The secondary current wave-form thereby suffers a displacement, and in addition the wave-form of the secondary current while it is rising and falling is altered from that occurring with no grid delay. Referring to Fig. 13b, it can be shown that the secondary current is now composed of the three current functions :—

$$i_1 = I_s(\cos\alpha - \cos\theta) \text{ from } \alpha \text{ to } \alpha + \mu_\alpha \quad (34)$$

$$i_2 = I_d \qquad \text{from } \alpha + \mu_\alpha \text{ to } \alpha + \frac{2\pi}{p} \quad (35)$$

$$i_3 = I_d - I_s\left\{\cos\alpha - \cos\left(\theta - \frac{\pi}{p}\right)\right\}$$

$$\text{from } \alpha + \frac{2\pi}{p} \text{ to } \alpha + \mu_\alpha + \frac{2\pi}{p} \quad (36)$$

where $I_s = \dfrac{I_d}{1 - \cos\mu_o}$ as given in Section II.

Fourier analysis of the secondary current wave-form made up of these three functions shows, as is to be expected, that the D.C. component is

$$I_{ms\alpha} = \frac{I_d}{p} \quad (37)$$

The expressions for the harmonic content are complicated and have no bearing on the present discussion. As in Section II, equating 'n' to unity in the harmonic expressions proves indeterminate and a different approach must be used.

From the output voltage wave-form as shown in Fig. 13a, a fairly simple calculation will show that the D.C. output voltage is

$$V_{d\alpha} = V_{do}\,\frac{\cos\alpha + \cos(\alpha + \mu_\alpha)}{2} \quad (38)$$

where V_{do} is rectifier *e.m.f.* given by equation 18.

Neglecting all losses, it is permissible to equate the total power carried by all secondary phases to the D.C. output power to give the *in-phase or power* component of secondary current at fundamental frequency as

$$I_{ls\alpha p} = I_d \cdot \frac{\sqrt{2}}{\pi} \cdot \sin\frac{\pi}{p} \cdot \frac{\cos\alpha + \cos(\alpha + \mu_\alpha)}{2} \quad (39)$$

Calculation of the reactive component is again by equation 27, using the correct current equations 34, 35 and 36, with the result that the *quadrature or reactive* component of secondary current of fundamental frequency is given by

$$I_{ls\alpha r} = \frac{I_d \cdot \sqrt{2}}{\pi} \cdot \sin\frac{\pi}{p} \cdot \left\{\frac{2\mu_\alpha + \sin 2\alpha - \sin 2(\alpha + \mu_\alpha)}{4\{\cos\alpha - \cos(\alpha + \mu_\alpha)\}}\right\} \quad (40)$$

Equations 39 and 40 correspond to equations 26 and 28 respectively and, as in these latter equations, they contain the common factor $\dfrac{I_d\sqrt{2}}{\pi}\sin\dfrac{\pi}{p}$ which is of course the fundamental component of secondary current calculated in Section I and given by equation 4. Hence, two further correction factors may be given :—

Power component correction factor

$$\omega(1\ \alpha)p = \frac{\cos\alpha + \cos(\alpha + \mu_\alpha)}{2} \quad (41)$$

Reactive component correction factor

$$\omega(1\ \alpha)r = \frac{2\mu_\alpha + \sin 2\alpha - \sin 2(\alpha + \mu_\alpha)}{4\{\cos\alpha - \cos(\alpha + \mu_\alpha)\}} \quad (42)$$

To appreciate the true significance of these equations a series of curves has been drawn and will be explained in the next sub-section. It should, however, first be noted that the angle of overlap μ_α is different from that under no grid delay. The relation between μ_α and μ_o for different values of α is given by $\cos(\alpha + \mu_\alpha) = \cos\alpha + \cos\mu_o - 1$. (43)

Since μ_o is the quantity generally known, a series of curves is presented in Fig. 15 which allows μ_α to be obtained from μ_o for any value of grid delay.

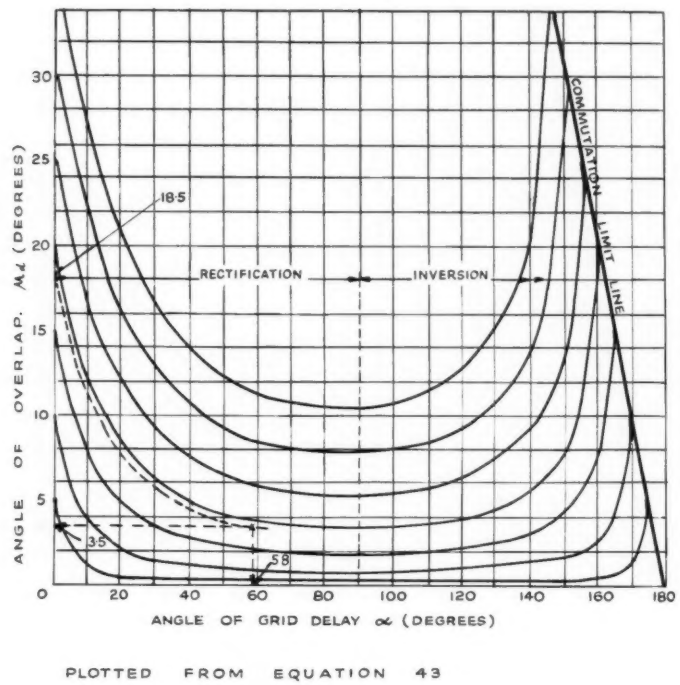

Fig. 15.—Variation of angle of overlap with grid delay

To understand the curves in Fig. 16, first consider a theoretical case of grid control of an equipment having an A.C. reactance of zero. Let the equipment be feeding a motor load which can carry a constant current in one direction and yet change its voltage from one direction to zero and then reverse it. This means, of course, that the motor is accepting power in one case and delivering power in the other.

With α equal to zero the D.C. voltage is a maximum and the power component of the fundamental is also a maximum while its reactive component is zero and the displacement angle is zero. As α is increased to 90° the D.C. voltage reaches zero, as does the power component, while the reactive component reaches the maximum. The displacement also reaches 90°. An increase of α to 180° causes the D.C. voltage and the power component to reach their maximum in the reverse direction, while the reactive component is back to zero and the displacement is 180°.

Since the current is maintained unidirectional during the change of voltage there must be a reversal of power, *i.e.* the rectifier acts as a deliverer of power to the D.C. side until the voltage reaches zero, after which it accepts power from the D.C. side and so becomes an 'inverter.' It was seen in Section I under 'A.C. Component of Fundamental Frequency' that the displacement of the fundamental component of secondary current is also a measure of power factor. Hence the power factor of a grid-controlled rectifier is easily calculated as cosine $\gamma_{1s\alpha}$.

When the practical case of A.C. reactance is allowed for as well as grid delay, conditions are modified, as has been seen in Section II, by the fact that A.C. reactance in itself demands reactive kVA. The group of curves in Fig. 16 show how the various quantities are influenced by grid delay and

Significance of Secondary Current Analysis

The components of the secondary current calculated in the previous sub-section can be applied to the equivalent diagram as was done in Section I.

D.C. COMPONENT

The D.C. component retains, as it must, the same value as in the 'Simple Rectifier Theory' as well as in the case where overlap was introduced.

A.C. COMPONENT OF FUNDAMENTAL FREQUENCY

In Fig. 16 the two correction factors $\omega\,(1\ \alpha)p$ and $\omega\,(1\ \alpha)\,r$ are plotted in terms of α for different values of μ_α. A further very interesting factor, namely the phase displacement of the fundamental component from the secondary voltage $E_{S\mu}$, is given as calculated from

$$Tan\ \gamma = \frac{2\mu_\alpha + \sin 2\alpha - \sin 2\,(\alpha + \mu_\alpha)}{\cos 2\alpha - \cos 2\,(\alpha + \mu_\alpha)} \quad . \quad (44)$$

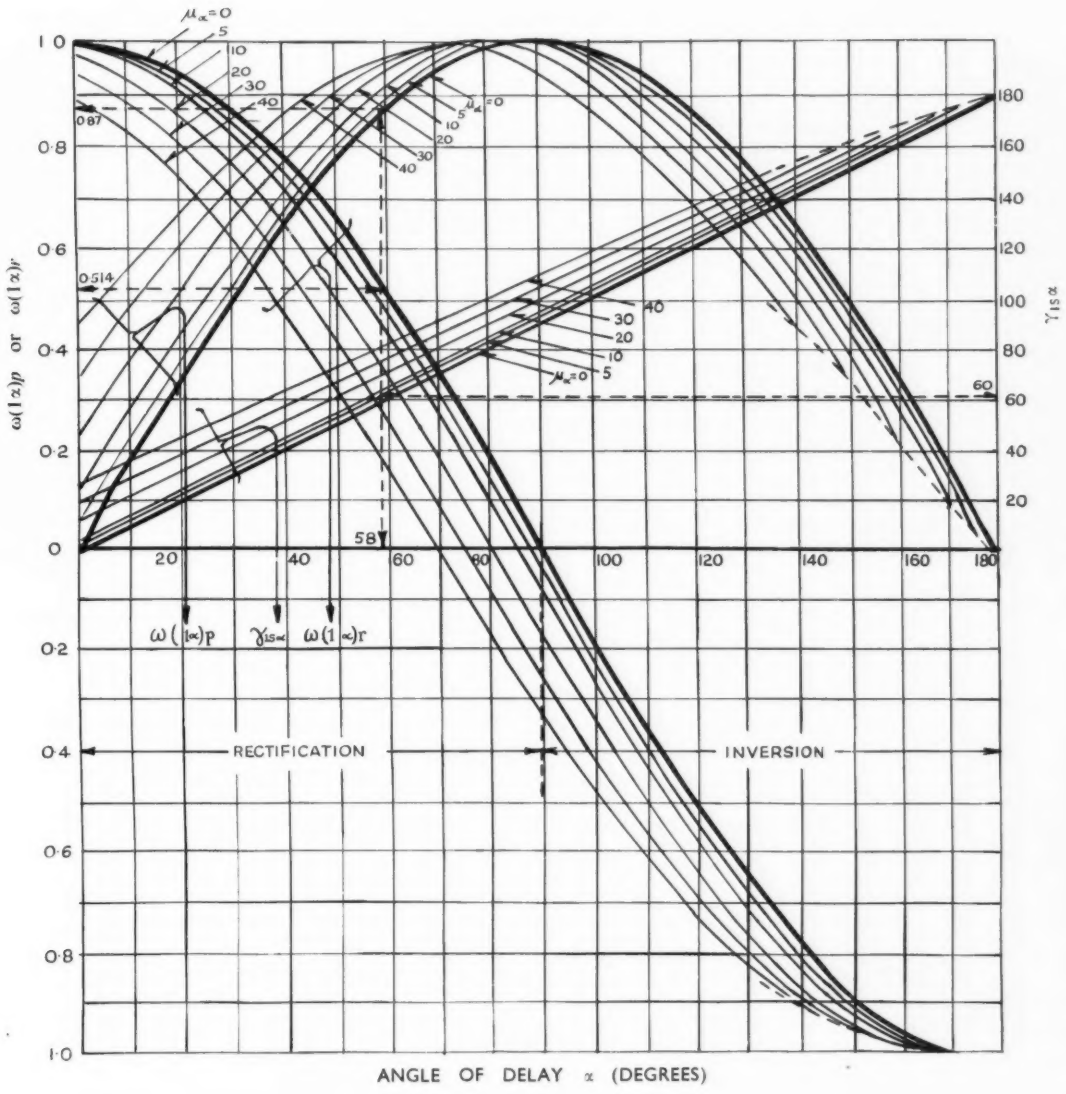

Fig. 16.—Variation of power component, reactive component and phase of fundamental component of secondary current, with angle of delay and overlap

TABLE VIII

EXAMPLE OF POWER BALANCE

$p = 3 \quad m = 4 \quad k = 4$

Quantity	Equation	Reference	Example
D.C. power output	$P_{d\alpha} = V_{d\alpha} \cdot I_{dc}$	—	2,500 kW
D.C. voltage	$V_{d\alpha}$	—	250 volts
Direct current	I_{dc}	—	10,000 amp
Angle of grid delay	α	—	58°
Angle of overlap ($\alpha = 0$)	μ_o	—	18·5°
Angle of overlap ($\alpha = 58°$)	μ_α	Fig. 15	3·5°
Increment of D.C. voltage for losses	$\Delta V_{dc} = \frac{P_{cu} + P_{arc}}{I_{dc}}$	Eqn. 33	28 volts
Total rectifier e.m.f.	$V_{do} = \frac{(V_{d\alpha} + \Delta V_{dc}).2}{\cos\alpha + \cos(\alpha+\mu_\alpha)}$	Fig. 16	541 volts
Secondary voltage	$E_{s\alpha} = \frac{V_{do}.\pi}{\sqrt{2}.p.\sin\frac{\pi}{p}}$	Eqn. 18	462 volts
R.M.S. fundamental component of secondary current (μ and $\alpha = 0$).	$I_{1so} = \frac{I_d\sqrt{2}}{\pi}\sin\frac{\pi}{p}$	Eqn. 4	975 amp
R.M.S. fundamental component of secondary current (power component, $\mu_\alpha = 3{\cdot}5°$)	$I_{1s\alpha p} = I_{1so} \cdot \omega(1\alpha)p$	Fig. 16 Eqn. 39	500 amp
R.M.S. fundamental component of secondary current (reactive component, $\mu_\alpha = 3{\cdot}5°$)	$I_{1s\alpha r} = I_{1so}.\omega(1\alpha)r$	Fig. 16 Eqn. 40	845 amp
Displacement of fundamental	$\gamma_{1s\alpha}$	Fig. 16 Eqn. 44	60°
Power factor	$\cos\gamma_{1s\alpha}$	—	0·50
Total secondary power	$P_{s\alpha} = m.p.I_{1s\alpha p}.E_{s\alpha}$	—	2,775 kW
R.M.S. fundamental component of primary current (power component).	$I_{1p\alpha p} = I_{1s\alpha_p}.\frac{E_{s\alpha}}{E_p}.K$	—	84 amp
Total primary power	$P_{p\alpha} = 3.I_{1p\alpha p}.E_p$	—	2,775 kW
R.M.S. fundamental component of line current (power component).	$I_{l\alpha p} = \sqrt{3}.I_{1p\alpha p}$	—	145 amp
Total line power	$P_{l\alpha} = 3.I_{l\alpha p}.\frac{E_p}{\sqrt{3}}$	—	2,775 kW

reactance. Before proceeding with an example to explain the result, it should be noted that allowance for copper loss and arc loss can be made by equation 33.

Practical Example

As an example it is proposed to take the equipment already considered as an example in the previous sections and assume that it is operating with some grid delay. All the conditions will be as assumed for the example in Section II with the addition that each control grid is delayed by an angle of 58°. A grid delay of 58° is chosen since in conjunction with the reactance drop and drop due to losses the D.C. voltage is reduced to 50%, a convenient value for the purpose of illustration. Table VIII shows the power balance, derived as before in Section II from equations developed in the text.

The curves given in Fig. 16 are of considerable interest as they enable calculation of the important power relations in grid controlled equipments and cover also the range of inversion.

Transformer Magnetising Current

In the calculation of power factor in the previous sections the magnetising current of the transformer was neglected. Although at full load this introduces little error in power factor, at light load it has a considerable influence. Calculation of power factor allowing for magnetising current is easily made by using information calculated in the previous sections.

Corrected power factor for a primary magnetising current of I_e :—

$$\text{Cos } \gamma_{1p\mu c} = \frac{I_{1p\mu p}}{\sqrt{\{I^2_{1p\mu p} + (I_{1p\mu r} + I_e)^2\}}} \quad . \quad (45)$$

for conditions as in Section II, and

$$\text{Cos } \gamma_{1p\alpha c} = \frac{I_{1p\alpha p}}{\sqrt{\{I^2_{1p\alpha p} + (I_{1p\alpha r} + I_e)^2\}}} \quad . \quad (46)$$

for conditions as in Section III.

Power factor calculated by the above equations

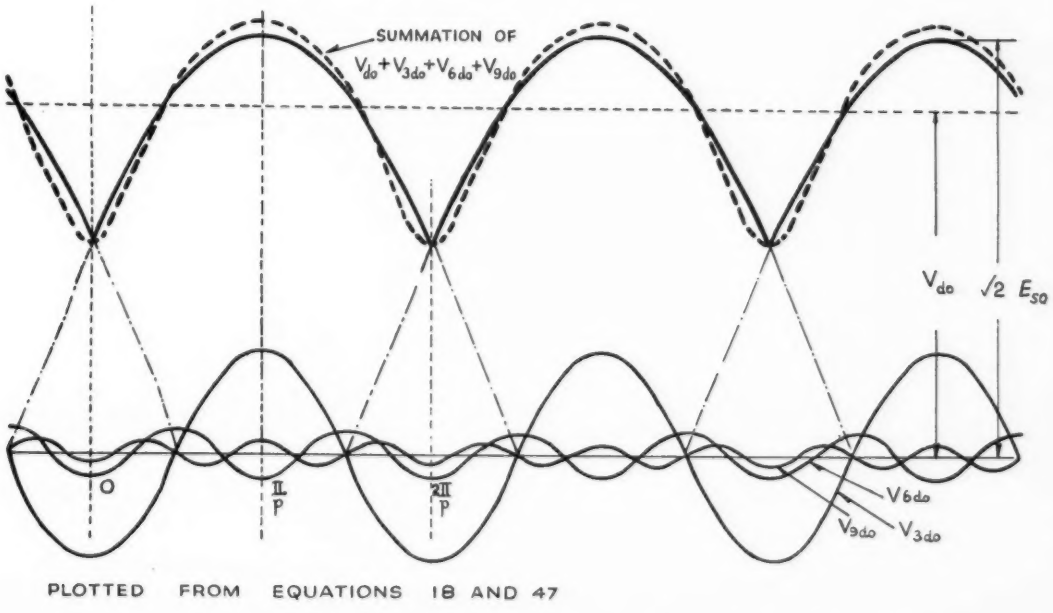

Fig. 17.—Harmonic analysis of output voltage wave for p = 3

is the displacement factor in line with the requirements of B.S. 1698 : 1950. The values of $I_{Ip\mu_p}$, $I_{Ip\mu_r}$, $I_{Ip\alpha_p}$ and $I_{Ip\alpha_r}$ are calculated as given in the appropriate sections.

CONCLUSIONS

The purpose of this article has been to show that by analysing the secondary current wave-form it is possible to calculate many of the quantities required in rectifier operation. As an illustration of the procedure the problem of power flow has been considered, but similar reasoning can be applied to many other related problems involving rectifier operation.

While the hypothesis of infinite inductance in the D.C. side is maintained, the generation of harmonic currents on the A.C. system side and voltage harmonics on the D.C. side may be treated as separate problems. Once the more practical case of finite reactance in the D.C. side is taken into account, allowance has to be made for the circulating harmonic currents on the D.C. side and the manner in which their reflected components in the A.C. side combine with those already calculated on the basis of the theory of infinite inductance in the D.C. side. It can be shown that the harmonic currents flowing in the D.C. circuit, when reflected into the A.C. side and analysed into continuous functions, contain a fundamental component in

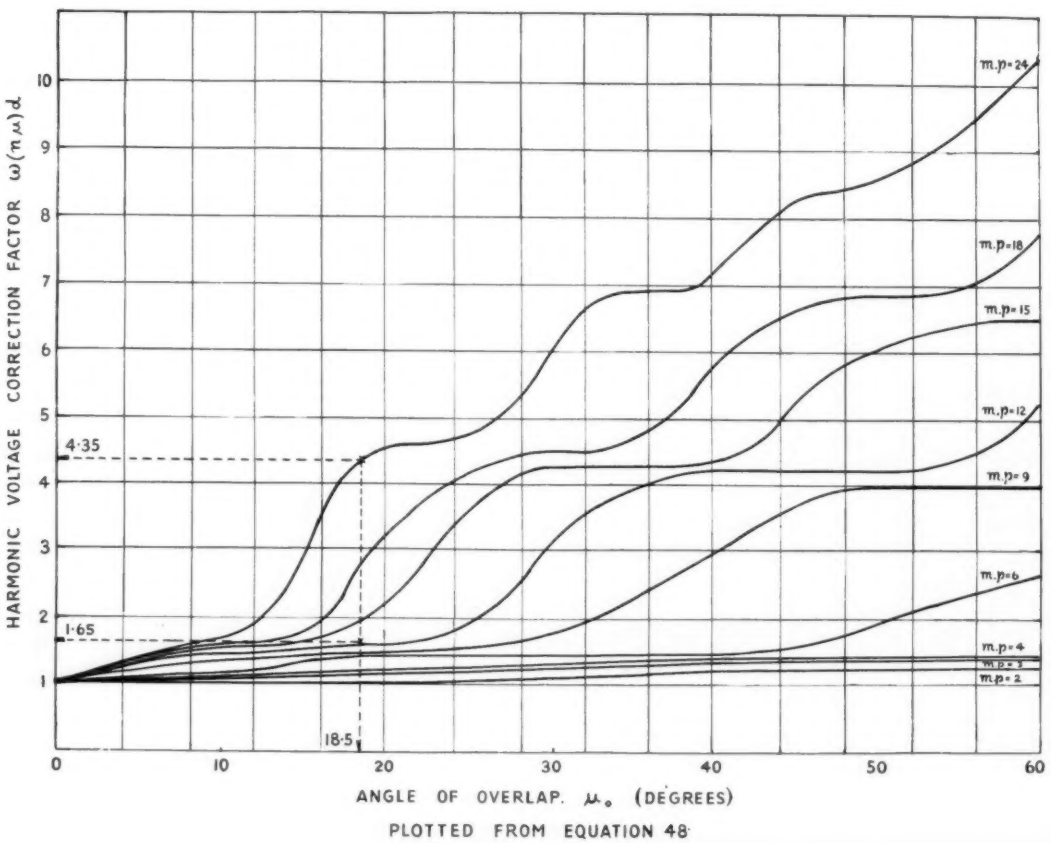

Fig. 18.—Overlap voltage harmonic correction factors

TABLE IX

R.M.S. value of n^{th} voltage harmonic (V_{no} as a percentage of V_{do})

n	$m.p = 2$	$m.p = 3$	$m.p = 4$	$m.p = 6$	$m.p = 12$	$m.p = 24$
1	—	—	—	—	—	—
2	47·1	—	—	—	—	—
3	—	17·7	—	—	—	—
4	9·4	—	9·4	—	—	—
5	—	—	—	—	—	—
6	4·1	4·1	—	4·1	—	—
7	—	—	—	—	—	—
8	2·2	—	2·2	—	—	—
9	—	1·7	—	—	—	—
10	1·4	—	—	—	—	—
11	—	—	—	—	—	—
12	1·0	1·0	1·0	1·0	1·0	—
13	—	—	—	—	—	—
14	0·7	—	—	—	—	—
15	—	0·6	—	—	—	—
16	0·6	—	0·6	—	—	—
17	—	—	—	—	—	—
18	0·4	0·4	—	0·4	—	—
19	—	—	—	—	—	—
20	0·3	—	0·3	—	—	—
21	—	0·3	—	—	—	—
22	0·3	—	—	—	—	—
23	—	—	—	—	—	—
24	0·2	0·2	0·2	0·2	0·2	0·2

addition to other harmonic components. Thus, should a rectifier operate with large harmonic currents in its D.C. side, for example, under heavy grid control, the values of the components of current calculated in this article need further modification.

In non-grid-controlled rectifiers, the harmonic voltages generated on the D.C. side are sufficiently low and the impedance of the D.C. circuit sufficiently high to allow only a small percentage of ripple current to flow. When grid control is used, conditions may be vastly different, in fact the vector sum of the harmonic currents in the D.C. side may exceed the direct current, *i.e.* the direct current becomes discontinuous. However, in practice large angles of grid delay are not used for long periods due to the bad influence of grid delay on power factor.

The theory developed in this article takes into account what may be termed the 'first order' modifications to simple theory to allow for practical operating conditions, *i.e.* allowances which must be made in the design of every equipment. However, there are further effects which sometimes have a significant influence on the operation of rectifier equipments but which only arise in certain instances; for example, A.C. system resonance, unbalanced and non-sinusoidal supply voltages and coupling between windings in a rectifier transformer. By applying further corrections to the developed theory the result of these 'second order' effects may be studied.

APPENDIX

Validity of Assumptions of Infinite D.C. Load Inductance

In the preceding sections due account has been taken of the assumptions upon which the simple theory of Section I was based, excepting that of infinite D.C. load inductance. It will be recalled that under this assumption the secondary current wave-form was always flat-topped, thus facilitating the harmonic analysis. In practice the load circuit has a finite inductance and it is therefore necessary to consider whether the change from infinite inductance to finite inductance will materially alter the conclusions already reached.

Although the degree of reliability of the expressions already derived may be ascertained by considering the time constant of the load circuit in relation to the dominant frequency in the D.C. voltage, no guide to an accurate solution is given by this method. Another method now given will lead to more accurate general solutions of the rectifier problem of loads with different impedances, and as the theory is somewhat complex the general line of approach only will be given.

Consider a simple rectifier circuit, as in Figs. 5 and 6, and calculate by Fourier analysis the various steady-state components of voltage which comprise the wave-form of the *D.C. output voltage*, i.e. the mean component and the harmonic components. Since the loads which a rectifier may feed can vary from electrolytic cells to series traction motors,

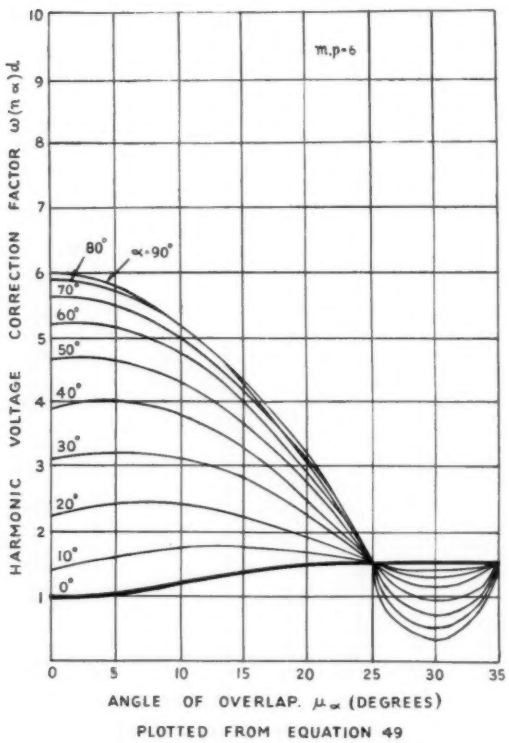

Fig. 19.—*Grid delay harmonic voltage correction factor for* $m.p = 6$

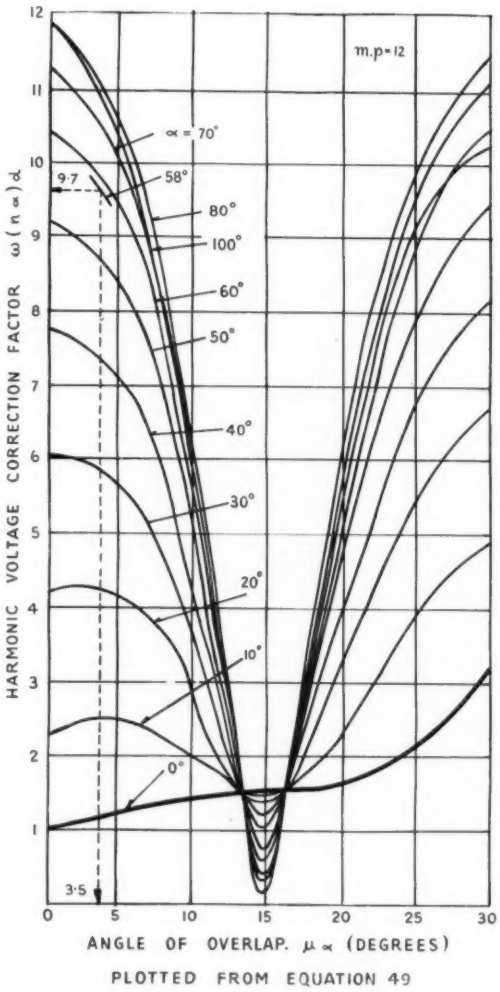

Fig. 20.—*Grid delay harmonic voltage correction factor for* $m.p = 12$

special treatment will be necessary in each case. For the sake of illustration consider a large D.C. machine load which is separately excited and has a sufficiently large inertia to prevent armature oscillation at the frequency of any harmonic in the output voltage of the rectifier. The mean D.C. voltage of the rectifier can in this case be treated as though it were present without any harmonic voltage, *i.e.* in line with the infinite inductance

TABLE X

EXAMPLE CALCULATION OF D.C. RIPPLE CURRENT

Quantity	Symbol	Reference	$m.p = 12$	$m.p = 24$
Rectifier e.m.f.	V_{do}	Table VII	541 volts	541 volts
Percent harmonic voltage ($\mu = o$) ..	$\%V_{ndo}$	Table IX	1·0%	0·2%
R.M.S. harmonic voltage ($\mu = o$) ..	V_{ndo}	—	5·4 volts	1·08 volts
Harmonic correction factor ($\mu = 18{\cdot}5$)	$\omega(n\mu)d$	Fig. 18	1·65	4·35
R.M.S. harmonic voltage ($\mu = 18{\cdot}5$)..	$V_{nd\mu}$	—	8·9 volts	4·7 volts
D.C. circuit impedance	X_{dc}	—	0·11 ohms	0·24 ohms
R.M.S. harmonic current	$I_{nd\mu} = \dfrac{V_{nd\mu}}{X_{dc}}$	—	81 amp	20 amp
Percent harmonic	$\%I_{nd\mu}$	—	0·81%	0·20%

theory, and the effect of harmonics can then be superimposed.

Application of the theory developed in the previous sections is therefore permissible but may need to be modified to allow for harmonics in the D.C. side.

The magnitude of the harmonic voltages will now be given for the three sets of assumptions in Sections I, II and III.

Voltage Harmonics in D.C. Side under Conditions of Section I

Fourier analysis of the wave-form in Fig. 6 shows that in addition to the mean component :—

R.M.S. value of n^{th} voltage harmonic

$$V_{ndo} = V_{do} \cdot \frac{\sqrt{2}}{n^2-1} \quad . \quad . \quad . \quad . \quad (47)$$

In table IX the values of these harmonics are given as a percentage of V_{do} for various values of $m.p$ (total number of phases in the output voltage). Consider the example in Table VI. V_{do} is 500 volts so that as $m.p$ for quadruple zig-zag connection is equal to 12, the 12th harmonic is 5 volts (500 × 1%) and the 24th harmonic is 1.0 volt (500 × 0.2%).

In Fig. 17 a particular case of $m.p$ equal to 3, as in Fig. 6, has been drawn to show that the combination of the mean D.C. voltages and harmonics in the right phase does sum up to the correct wave-form. The phase of each harmonic is derived during the calculation leading to equation 47 and is not given here as it has little bearing on the present argument.

Voltage Harmonics in D.C. Side under Conditions of Section II

The introduction of overlap causes a distortion of the D.C. voltage wave as shown in Fig. 12a from which analysis shows that the mean component (equation 25) and the voltage harmonics, as given in Table IX, are still all present although changed in value. The harmonics have increased in value according to a correction factor :—

R.M.S. value of n^{th} voltage harmonic

$$V_{nd\mu} = \frac{V_{do}\sqrt{2}}{n^2-1} \cdot \left[\frac{1}{2} \sqrt{ \left\{ (\cos n\mu_o + \cos \mu_o)^2 + (\sin n\mu_o + n.\sin \mu_o)^2 \right\} } \right] \quad . \quad . \quad (48)$$

where the term in the square brackets is called the harmonic voltage correction factor $\omega(n\mu)d$. In Fig. 18, $\omega(n\mu)d$ is plotted for a series of values of $m.p$ in terms of μ_o. As an example, consider Table VII in which V_{do} was 541 volts and the angle

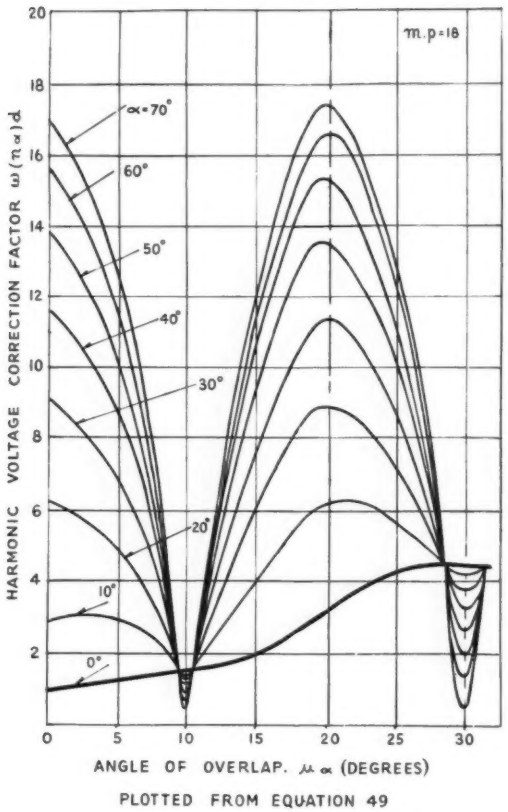

Fig. 21.—Grid delay harmonic voltage correction factor for m.p = 18

of overlap μ_o equal to 18.5°. Assume that the total inductance of the D.C. circuit including rectifier transformer, D.C. reactor and load is 0.03 millihenries, and calculate the harmonic current which will flow due to the harmonic voltages, expressing this as a percentage of the direct current[3]. Table X shows the calculated harmonic percentage, from which it is seen that, assuming the two major harmonics are in phase, the total ripple is only 1.0%. Therefore, in this example, it is safe to say that the assumption of infinite D.C. inductance is sufficiently valid, since the ripple current set up in the D.C. circuit is a small percentage of the total direct current.

In general, for equipments where grid control is not used, the assumption of infinite D.C. inductance is permissible and therefore the results derived in previous sections are valid. The example chosen

[3] *The inductance of the circuit in which the harmonic currents flow is made up of an equivalent rectifier transformer inductance, possibly a series reactor, busbars and load inductance. For the double star or quadruple zig-zag connection the equivalent inductances of the rectifier transformer can be calculated from :—*

$$L_T = \%\, X_c \cdot \frac{V_{do}}{I_{dc}} \cdot \frac{1}{9.2\pi} \text{ millihenries} \quad . \quad . \quad . \quad (49)$$

This equation gives L_T = 0.019 millihenries in the above example, and an allowance of 0.011 millihenries has been made for the remainder of the circuit.

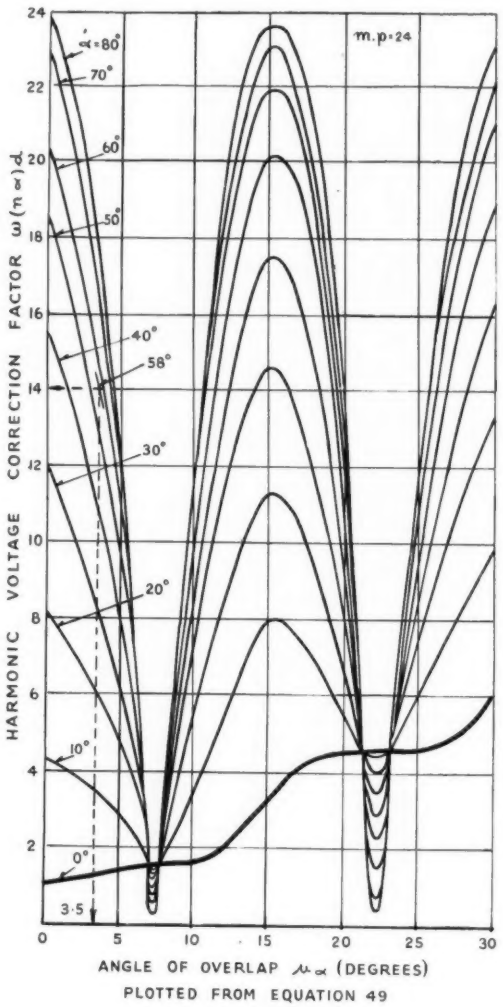

Fig. 22.—Grid delay harmonic voltage correction factor for m.p = 24

may be considered somewhat ideal as it has a low voltage, large current and large number of phases, but calculation of other equipments shows that the ripple current does not become sufficiently large to invalidate the theory. Special cases exist, such as bi-phase, where special measures of calculation have to be used.

Grid control, as shown in Fig. 13a, is responsible for further distortion of the D.C. voltage with a consequent increase in the harmonic voltages and current.

Voltage Harmonics in D.C. Side under Conditions of Section III

Analysis of the complex voltage wave-shape given in Fig. 13a results in the following solution for the harmonics, while the mean component is as given by equation 38.

R.M.S. value of n^{th} voltage harmonic

$$V_{n\alpha} = V_{do} \cdot \frac{\sqrt{2}}{n^2-1} \cdot \omega(n\alpha)d \quad . \quad . \quad (50)$$

where $\omega(n\alpha)d = \sqrt{\left[(n-1)^2 \cdot \cos^2 \left\{(n+1)\ \tfrac{1}{2}\mu_\alpha\right\} + (n+1)^2 \cdot \cos \left\{(n-1)\ \tfrac{1}{2}\ \mu_\alpha\right\} - 2(n-1)(n+1) \cdot \cos \left\{(n+1)\ \tfrac{1}{2}\mu_\alpha\right\} \cdot \cos\left\{ (n-1)\ \tfrac{1}{2}\mu_\alpha\right\} \cdot \cos (2\alpha + \mu_\alpha)\right]}$

where the correction factor for overlap and grid delay $\omega(n\alpha)d$ is the complete term within the root sign. To illustrate the manner in which this factor varies with 'μ_α' and 'α', sets of curves are given in Figs. 19, 20, 21 and 22 for the 6th, 12th, 18th and 24th harmonics respectively. Now consider the example taken in Section III and tabulated in Table VIII. V_{do} is 541 volts, α is 58° and μ_α is 3.5° so that the current ripple in the D.C. circuit can be calculated as in Table X, but using the curves in Figs. 20 and 22 instead of Fig. 18 to get the correction factors. The result is that the 12th harmonic current increases to 4.8% and the 24th harmonic to 0.6%, which assuming as before that they are in phase gives a total of about 5.4%. Obviously the secondary current wave-shape is not seriously distorted from that shown in Fig. 13b and on which Section III is based.

This example illustrates that even with large angles of grid delay the theory developed in Section III will generally apply. However, various combinations of harmonic voltages, direct currents, number of phases and harmonic impedance are possible. In any case where it is suspected that ripple current is large it can be checked as shown in this Appendix. As a general guide, if the R.M.S. ripple current does not exceed 10% of I_{dc} the theory developed in Section III is substantially correct.

The Property of Non-deterioration in the 'English Electric' H.R.C. Fuse Link

By E. JACKS, A.M.I.E.E., Fusegear Section.

One of the more important properties which has made the 'English Electric' cartridge fuse link a pre-eminent protective device, is that of non-deterioration. This is so because protective devices in service have to lie virtually dormant during most of their useful lives and to act only when a fault occurs. It has therefore become an established fact that the property of non-deterioration is of equal importance to any of the more active functions.

When the H.R.C. (high rupturing capacity) cartridge fuse link was first introduced, it was designed to satisfy two important, and at that time urgent, requirements. The first was rupturing capacity, to cope with the increasing fault levels on supply systems, and the second was non-deterioration to overcome the serious disadvantages suffered by the types of semi-enclosed fuses in common use at that time. The semi-enclosed fuse had proved itself to be unreliable and unable safely to interrupt the growing values of short-circuit current occurring on supply networks and factory installations. The position was made even worse by the fact that this type of fuse, consisting essentially of a piece of bare wire suspended in free air, was susceptible to rapid oxidisation and premature failure when carrying normal load currents. This gave rise to considerable abuse by encouraging users to strengthen the fuse wire, thus nullifying the effectiveness of the fuse as a protective device. Otherwise the interruptions in supply due to premature fuse blowing caused considerable inconvenience, and quite often loss of production. The fully-enclosed cartridge type fuse was born of necessity and has provided the solution to these and many other problems. Non-deterioration was and still is one of its most valuable attributes.

This was fully realised in the early stages of development of the 'English Electric' H.R.C. fuses some twenty-five years ago, when measures were adopted to ensure that the fuse would maintain constant characteristics throughout its working life. How well this policy was implemented has been amply illustrated by recent tests which have been carried out on cartridge fuses which have been in use for periods of up to twenty-five years. These tests are the culmination of other similar tests which have been carried out from time to time, and were made possible by the co-operation of the North Western Electricity Board of the British Electricity Authority who supplied fuse links which had been in service in their own substations. They were also able to supply data to substantiate the histories of the fuse links with regard to loading and other service conditions.

The tests described in this article are unique in that The English Electric Company is one of the very few concerns in the world which have been manufacturing fuse links for a sufficiently long period to provide data for an actual life test of over a quarter of a century. Although enclosed fuses of various types had been in use early in the century, the modern conception of the high rupturing capacity cartridge fuse link is a British development which was pioneered to a very large extent by this Company.

The word 'non-deterioration' is one which has become identified by usage with H.R.C. fuse practice; it describes a characteristic property which has been proved in service by millions of 'English Electric' fuses since they were introduced over twenty-five years ago. The results of the tests now provide documented evidence that for all

practical purposes a complete degree of non-deterioration has been achieved.

The question of non-deterioration is primarily one of preventing changes in the constituent materials of the fuse, but the problems involved in achieving the desired result cannot be so simply stated. Although the H.R.C. fuse is a static piece of equipment, it performs an active function in that it carries load currents of varying degrees throughout its life, and from time to time may have to withstand through-fault currents of considerable magnitude. It is subject to external influences which may vary from normal ambient conditions in clean atmospheres, to extremes of temperature and atmospheric contamination as well as mechanical strain due to the vibration of associated

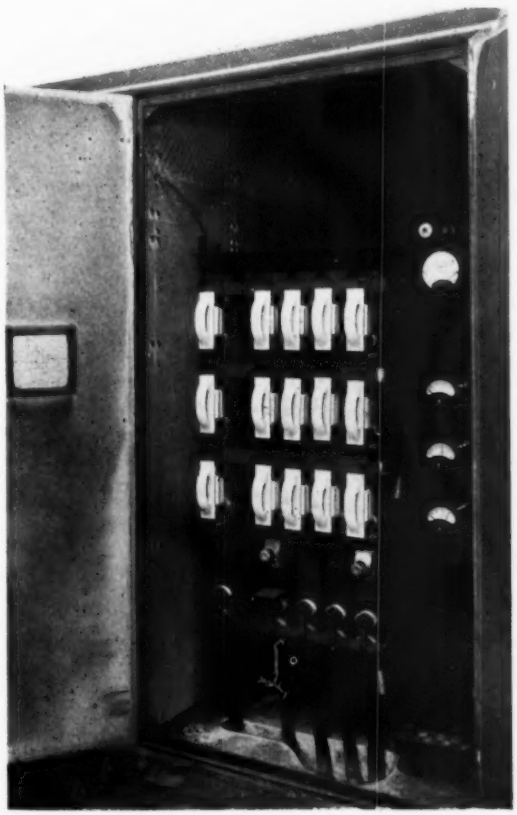

Fig. 1.—*Bromiley Cross Kiosk, installed* 1927

Fig. 1a.—*Close view of fuse assembly in Bromiley Cross Kiosk*

equipment or adjacent machinery. In addition, it must be ready and capable at all times of safely interrupting short-circuit currents of all magnitudes up to the maximum fault level of the system in which it is installed. This latter condition provides the most stringent test of all.

When a fuse is interrupting a short-circuit current of a value normally to be expected under present-day conditions, it is controlling large values of potential power and is being subjected to a high degree of strain. It is under such strain that any changes or weaknesses will show themselves, and the smallest change from original condition may be magnified many times under fault conditions. Between the two extremes of normal load and fault conditions the fuses may have to handle many values of over-current due to overload and through-fault current, and will have to discriminate with other protective devices. For this purpose cartridge fuses are manufactured to conform to published time/current characteristic curves to which they must remain faithful throughout their

working lives. Non-deterioration is thus related to every function which the fuse has to perform and every condition which it has to meet in service.

It will be seen that although the H.R.C. fuse as a protective device is simple in conception, its duties are both wide and complex, and its performance must be such as to cover satisfactorily the increasingly varied contingencies which arise in service.

Fuse design has undergone several changes since the H.R.C. cartridge fuse was first introduced. During the last decade particularly, fault conditions have increased in severity and fuse performance has had to be stepped-up to meet them. As a result, non-deterioration is more important than ever. An examination of the performance data of present-day fuses, which are described towards the end of this article, will show that the tolerances allowable in all aspects of manufacture are being held to closer and closer limits. This applies not only to dimensional tolerances but also to the selection and grading of materials. The degree of non-deterioration must be of the highest order to ensure proper functioning of the fuse under the fault conditions which may occur years after it has left the factory.

Selection of Fuses for Non-deterioration Tests

The degree of non-deterioration in a particular design of fuse is difficult to assess because the only genuine trials are those of actual service. It is necessary to wait for a considerable number of years before being able to prove non-deterioration beyond all doubt. Such a period having passed since the ' English Electric ' cartridge fuse was first introduced, steps were taken to carry out the appropriate tests.

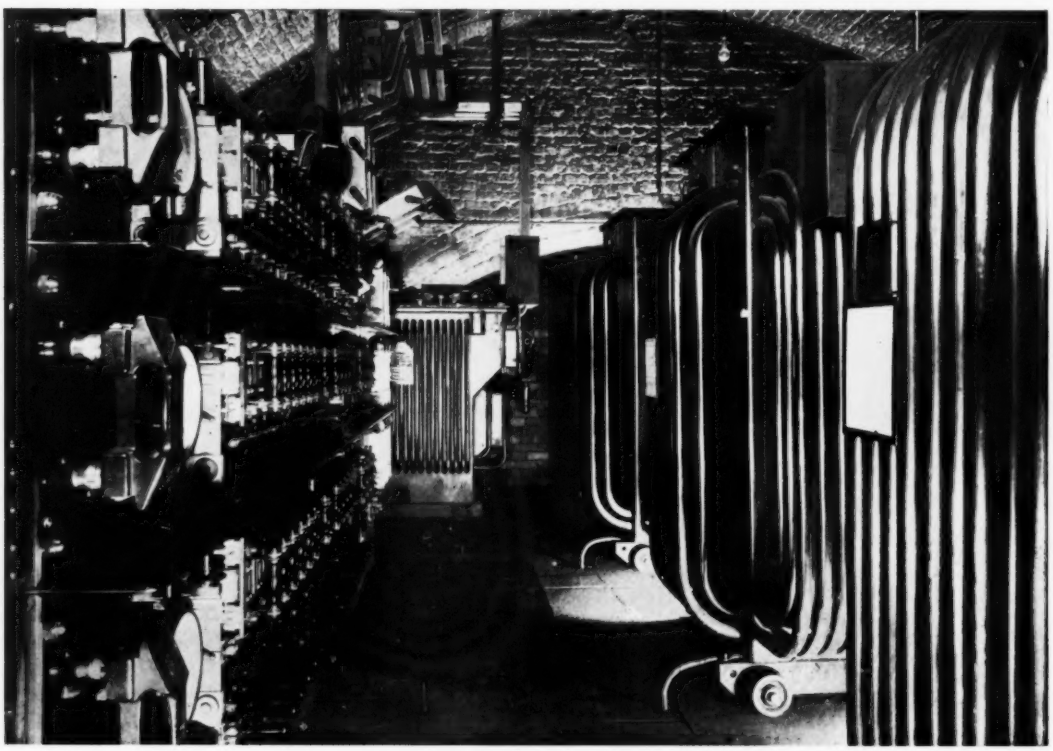

Fig. 2.—Market Hall Substation, Bolton, installed 1934

A search was made for suitable fuses which were known to have been in service for the required period and whose histories could be vouched for accurately and with certainty. Of the many possibilities which presented themselves, it was decided to accept the generous offer of assistance from the North Western Electricity Board, on whose system were many fuses which were known to have remained in service unchanged for periods of eighteen to twenty-five years. A substantial number of fuse links were taken from seven selected substations, each of which represented a different type of load, including heavy industrial, commercial, and domestic. Each of these substations had been under the direct supervision of the same engineer since they were first commissioned, and it was possible to obtain a personal guarantee from the engineer concerned that the fuses had remained undisturbed since they were first installed. In addition, it was possible to obtain a reasonable estimate of the ampere loadings to which the fuses had been subject both in winter and in summer during their years of service. Careful notes were also made of the ambient atmospheric conditions under which the fuses had been working.

The actual age of many of the fuse links was further checked by reference to the inspection marks which were put on the component parts of the cartridges during manufacture, and in some cases by noting small features of design which were known to be contemporary with the types of fuse manufactured at the time the selected fuse links were installed. By these means the accuracy of all data and periods of duty were checked beyond all reasonable doubt.

Table 1 gives a list of the fuse links selected, with brief details of site location, year of installation and loadings. The identification numbers allocated to the fuse links are used throughout the subsequent illustrations.

TABLE 1

SEVERITY OF SERVICE

Fuse Link Type and Identity Number	Location	Year of Installation of Fuse Link	Details of Loading
D.200F ND.100	Edgeworth Kiosk, No. 1 Circuit	1927	Summer— 50 amperes
ND.101 ND.102			Winter— 100 amperes
D.200F ND.103 ND.104 ND.105	Edgeworth Kiosk, No. 2 Circuit	1927	Summer— 50 amperes Winter— 100 ,,
D.200F ND.106 ND.107 ND.108	Bromiley Cross Kiosk	1927	Summer— 50 amperes Winter— 100 ,,
D.200F ND.109	Harwood Kiosk	1927	Summer— 50 amperes Winter— 100 ,,
28T250F ND.110 ND.111	Market Hall Substation, No. 3 Circuit	1934	Summer— 125 amperes Winter— 210 ,,
28TK300 ND.112	Market Hall Substation, No. 3 Circuit	1934	Summer— 150 amperes Winter— 250 ,,
29T300K ND.113 ND.114 ND.115	Market Hall Substation, No. 1 Circuit	1934	Summer— 150 amperes Winter— 250 ,,
30T350M ND.116 ND.117 ND.118	Market Hall Substation, No. 2 Circuit	1934	Summer— 175 amperes Winter— 300 ,,
TM400 ND.119 ND.120 ND.121	Weaste Road South Substation, No. 1 Feeder	1935	1935— 100 amperes 1939— 230 ,, 1952— 250 ,,
TM400 ND.122 ND.123 ND.124	Weaste Road South Substation, No. 2 Feeder	1935	1935— 120 amperes 1939 to 1952— increase to 300 amperes
TM400 ND.125 ND.126 ND.127	Gore Avenue Substation, Weaste Lane West Side	1935	1935— 50 amperes 1942— 150 ,, 1952— 200 ,,
TM400 ND.128 ND.129 ND.130	Gore Avenue Substation, Weaste Lane East Side	1935	1935— 50 amperes 1942— 150 ,, 1952— 200 ,,
TKF.300 ND.131 ND.132 ND.133	Bolton Street Substation	1936	Summer— 150 amperes Winter— 250 ,,

NOTE.—All substations subject to peak winter overloads.

Figs. 1, 2 and 3 show interior views of some of the substations from which the selected fuse links were taken, and indicate in some measure the conditions under which they worked in service.

The steel kiosk type substation shown in Fig. 1 serves a domestic and rural network and was commissioned prior to 1927. A close view of one of the fuse handles and contacts is shown in Fig. 1a, and it will be seen that this equipment has acquitted itself well, remaining in excellent condition over a period of twenty-five years and showing promise of good service for many years to come.

The fuse links selected from this location were of 150 amp rating (in accordance with B.S. 88 : 1952), and were of a type which was so old as to have become obsolete in general design almost twenty-five years ago. They nevertheless embodied all the features relevant to the study of non-deterioration. The fuses had carried loads varying between 50 and 100 amp with peaks of higher value during winter conditions. It was difficult in this case to obtain accurate data concerning the actual value of the highest winter loads, but it is estimated that these would have exceeded 150 amp during extremely cold periods.

The substation fuse board shown in Fig. 2 is of very old design which had been specially adapted to accommodate the then newly introduced cartridge fuses. The ambient temperatures in this substation were fairly high due to a consistently high town load, and certain difficulties in substation ventilation. The fuses selected for test were of both 300 and 350 amp capacity and for 18 years had carried winter loads of 250 amp and 300 amp respectively, and summer loads of 150 amp and 175 amp respectively, both with peaks of overload during very cold or severe weather.

The substation fuse board shown in Fig. 3 is of the 'English Electric' Skeltag design serving a mixed industrial and domestic load and subject to a considerable degree of atmospheric polution. The fuses selected in this case were of 400 amp

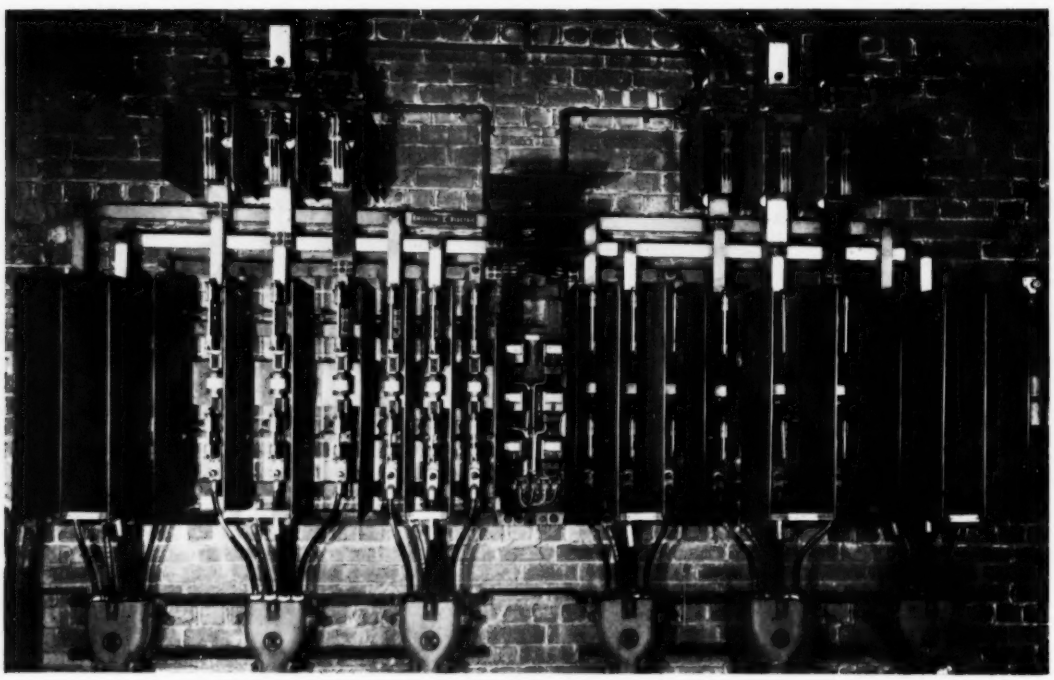

Fig. 3.—Weaste Road South Substation, Salford, installed 1935

capacity and had carried loads increasing from 100 amp in 1935 to 250-300 amp in 1952, again with winter overloads which it is estimated would sometimes have exceeded the nominal rating of the fuses for short periods. It is also considered inevitable that all the selected fuse links would at some time or other have carried through-fault currents due to faults on branch networks or on consumers' installations.

Investigation to Determine Physical and Electrical Condition of the Selected Fuse Links

The 'English Electric' fuse link consists principally of a ceramic body, pure silver elements, clean silica quartz, asbestos washers, porcelain plugs, brass end-caps and copper tags, the last two items being electro-tinned. The assembly also includes solder of various types, cement and indicator devices. Deterioration must involve a change in one or more of these materials or a change in their structure, and the tests described were devised to explore every possible aspect of the factors involved.

A total of 34 fuse links was available for investigation, and as some of the tests and examinations contemplated involved the blowing or dismantling of some of the samples at various stages, the programme was arranged to ensure that a full complement of tests was carried out on each type of cartridge.

In order to provide a basis of comparison in each of the tests, a number of fuse links were made up exactly to the specification which obtained when each type of those under test was originally manufactured, and great care was taken to use the identical materials originally used and to follow the original methods of manufacture. The programme was then so arranged that the old and new fuses could be tested simultaneously whenever possible. This enabled the comparisons obtained to be checked and studied at each stage.

The testing programme resolved itself into the investigation of electrical performance, preceded by resistance measurements and a thorough physical examination. These may be arbitrarily listed as follows :—

(*a*) Visual exterior examination.
(*b*) Radiograph examination.
(*c*) Visual interior examination, including examination of each component part.
(*d*) X-ray difraction tests of constituent materials.
(*e*) Measurement of fuse link resistance.
(*f*) Temperature rise tests at full rated current.
(*g*) Determination of minimum fusing currents.
(*h*) Short-circuit tests at various critical values of prospective short-circuit current.

Visual Condition of Selected Fuse Links

The external condition of the selected fuse links, some of which are shown in Fig. 4, indicates the effect of atmospheric conditions on the fuse caps, tags and ceramic bodies. The illustration shows the selected fuses compared with similar fuses of new construction.

It will be seen that the contact surface on the fuse tags has been maintained in good condition in all the examples.

In contrast to the contact surfaces, the end caps of the selected fuse links show various degrees of oxidisation and surface contamination, which in each case is consistent with the atmospheres and ambient conditions in which the fuses have been working.

All soldered joints between tags and end caps are good, the ceramic bodies are unimpaired, and the cement joints are as effective as when the fuses were new.

Examination by Radiography

All the selected fuse links were radiographed, and Fig. 5 shows the X-ray plates corresponding to the fuse links illustrated in Fig. 4. As before, the plates are arranged in sets to show a comparison between the old and new fuse links of similar construction. The undisturbed interior condition of the fuse links can be quite clearly seen. By careful interpretation it is possible to check that the gap portion of each element is adequately spaced from the others, and it is in every case properly positioned at the centre of the fuse link body. It will also be seen that there has been no thinning of the elements due to corrosion, or sagging due to mechanical or thermal stress.

Visual Condition of Interior Components

Fig. 6 shows two examples from the selected fuse links with the outer end caps removed. It will

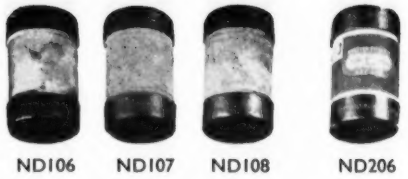

ND106 ND107 ND108 ND206

(BROMILEY CROSS KIOSK)

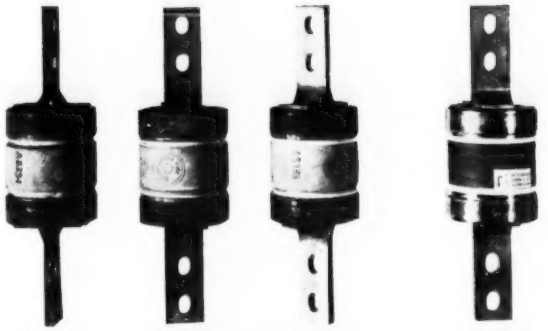

ND125 ND126 ND127 ND224

(GORE AVE. SUBSTATION WEST SIDE)

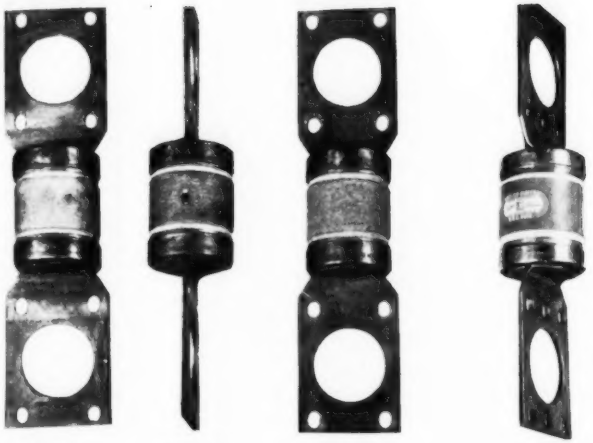

ND113 ND114 ND115 ND203

(MARKET HALL SUBSTATION No. 1 CIRCUIT)

ND131 ND132 ND133 ND231

(BOLTON ST. SUBSTATION)

Fig. 4.—Fuse links as taken from service and compared with new fuse link of similar construction. Scale one-quarter full size

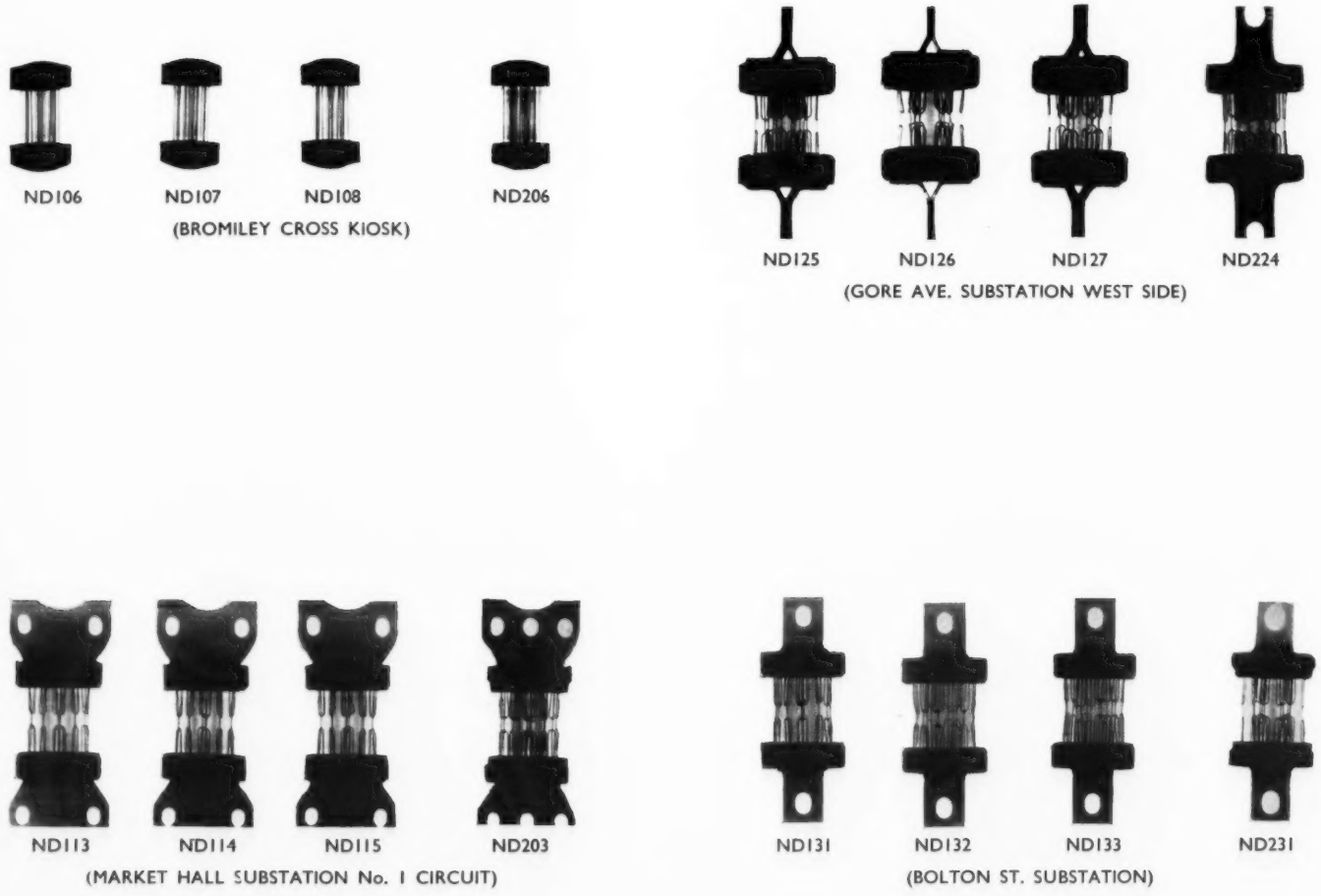

Fig. 5.—Radiographs of the fuse links shown in Fig. 4

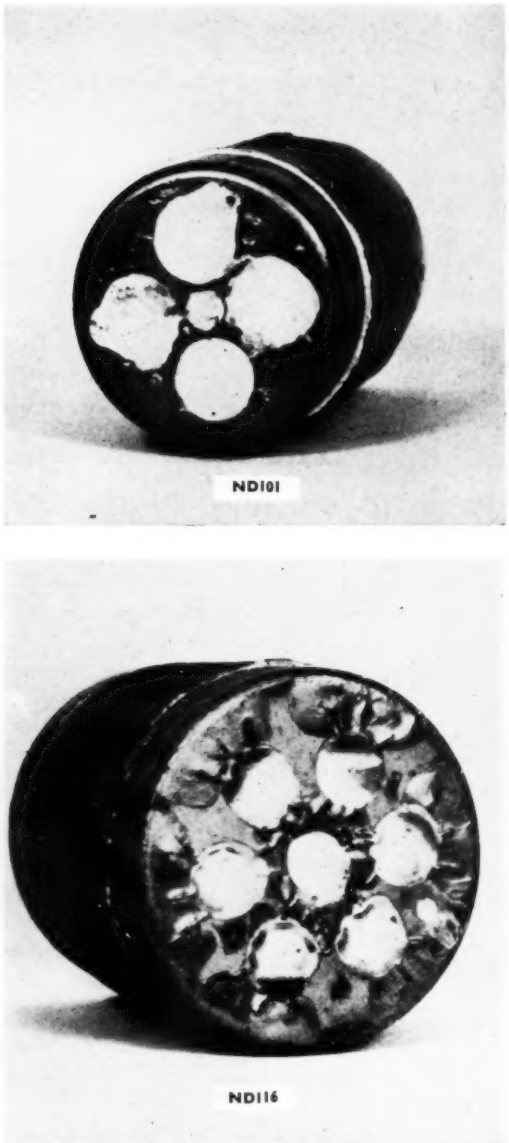

Fig. 6.—End views of two samples of fuse links with outer caps removed, showing condition of sealing, plating and soldering

be seen that the outer end caps are solidly soldered to the inner end caps, and the silver elements are in turn each soldered to the inner end cap. It is considered that dry joints should be permitted only in positions where they can be checked periodically or when large enough and solid enough to be beyond doubt. The internal connections of the fuse link do not come within this category, as they are hidden out of sight and are therefore out of mind. Fig. 6 shows the conditions of the soldered joints and is evidence of how this design feature has been implemented with success.

The advantage of soldering the elements to the inner end caps is that the solder makes a perfect electrical contact without affecting the structure of the materials being joined together. Other methods of making the connection, such as welding, tend to reduce the cross section of the elements and to distort the surface to which the elements are joined. It is for this reason that the welding of elements (by methods at present available) is to be deprecated.

The hermetic sealing of the elements within the cartridge is seen in Fig. 6 to have remained completely effective. The cement seals show no sign of disintegration, a remarkable achievement when it is considered that the fuse link, as a thermal device, has been subject to innumerable temperature cycles, involving expansions and contractions of the end caps and cement alike, over a long period of years.

The internal components of the same cartridges are shown in Fig. 7. The silver elements are seen to be as bright as in their pristine condition. The ceramic plugs and asbestos washers are in good condition and the quartz filler is completely unchanged. A test for moisture content of the internal parts also showed that there had been no significant absorption of moisture by any of the materials concerned.

The examination of the fuse elements also included a photo-micrograph examination. Fig. 8 shows a series of plates which again provide comparisons between the old and the new elements. It will be seen from both the sectional and longitudinal profiles that there is no evidence of surface erosion. The plates showing the sections of soldered joints also prove that no change has taken place in the contact between the solder and the silver elements. A true soldered joint should give completely intimate contact without affecting the surface of the metal to which the solder is attached.

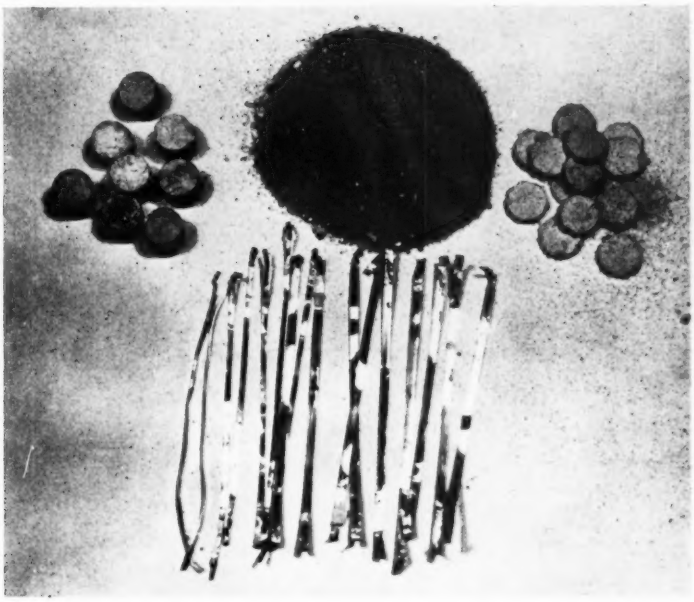

Fig. 7.—Internal components of the fuse links shown in Fig. 6, comprising elements, filler, sealing washers and ceramic plugs

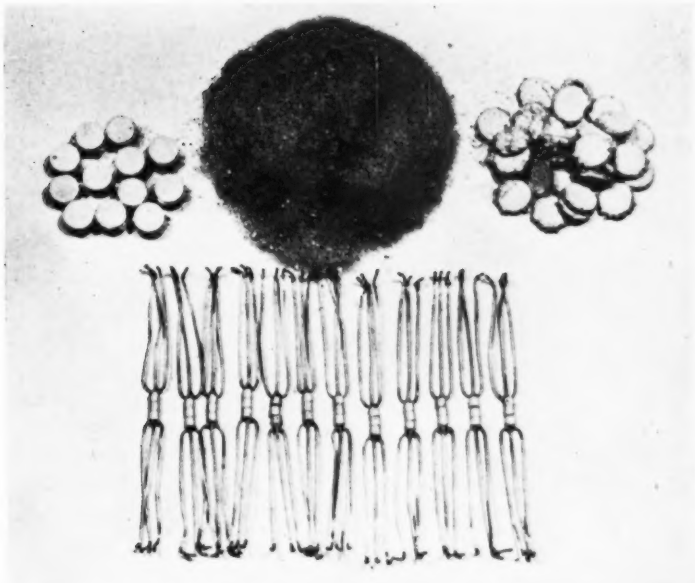

This result has been successfully achieved on each of the samples submitted for examination, and no change could be detected in the effectiveness of any of the joints. It can be seen that the mixture of solder has been varied slightly between the old and the new elements, but this has no significant bearing on the factors affecting deterioration. For those to whom this method of presentation is not familiar it may be useful to explain that the horizontal wire shown on each of the soldered joints is actually a transverse section through a curved circular wire. This gives the appearance of narrowing towards the middle, but it will be appreciated that this is a function of the method by which the wire has been cut and that the actual wire has not been reduced in section.

X-ray Diffraction Tests

Another method which was tried in an effort to detect changes in the fuse elements was that involving X-ray diffraction tests, which were carried out on an experimental basis in the spirit of 'leaving no stone unturned.' It was not expected that conclusive evidence could be obtained, as it is obvious that the only true basis of comparison would have been successive tests taken on the same pieces of material at the beginning and the end of the period under review. Although such a comparison was not possible, it was considered worth while to compare samples of silver taken from the old and new fuse links of similar construction.

The investigation failed to detect any significant change which might be interpreted as deterioration.

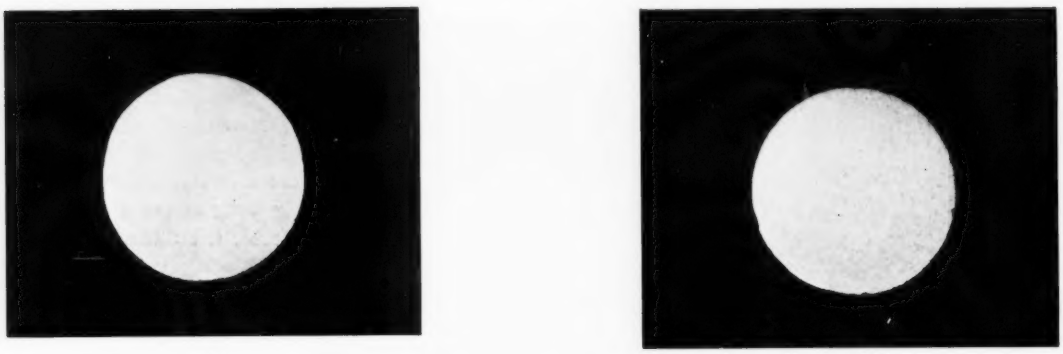

(a) (b)

TRANSVERSE SECTION OF GAP PORTION,
MAGNIFICATION × 70

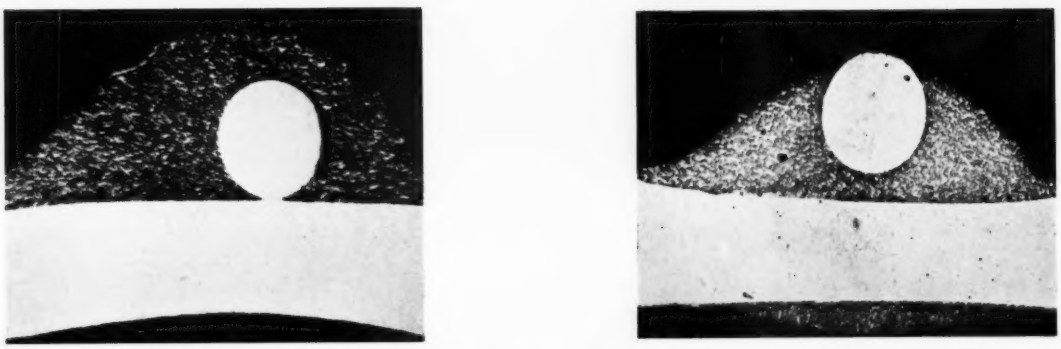

(a) (b)

TRANSVERSE SECTION OF SOLDERED JOINT,
MAGNIFICATION × 32

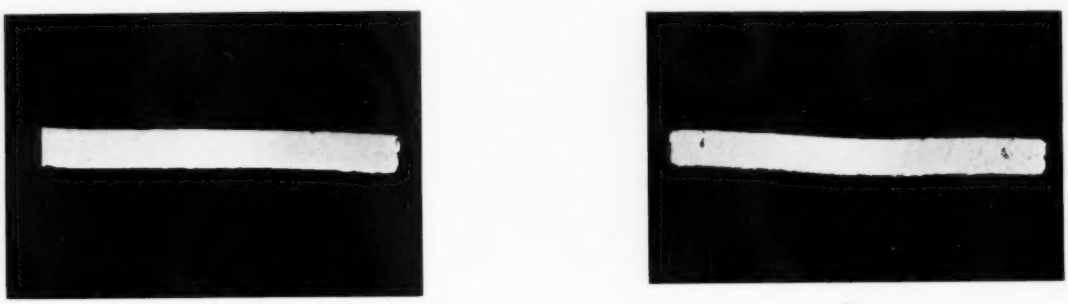

(a) (b)

LONGITUDINAL SECTION OF GAP PORTION,
MAGNIFICATION × 7

Fig. 8.—Photo-micrographs showing sectional and longitudinal profiles of silver elements

(*a*) *Sample taken from fuse link No. ND. 115 installed* 1934.

(*b*) *Sample taken from new fuse link of similar construction.*

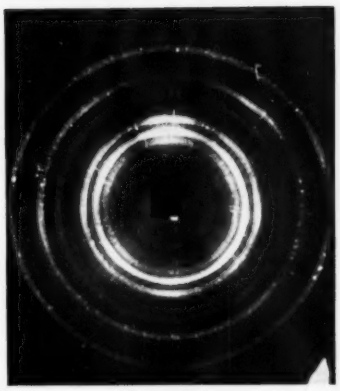

PLATE I
0·002 inch × 0·04 inch silver strip element.
of new construction.

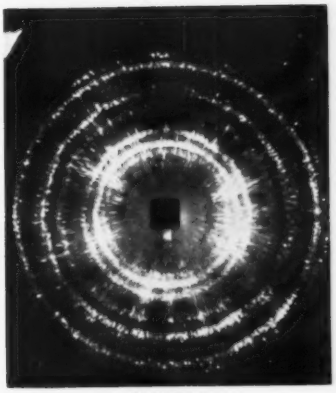

PLATE II
0·002 inch × 0·04 inch silver strip element.
After 25 years service.

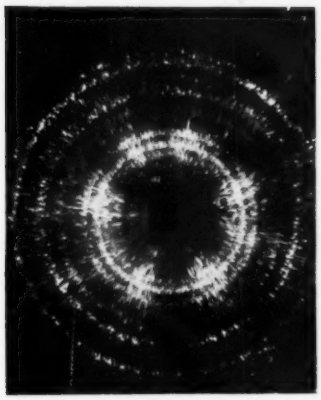

PLATE III
0·002 inch × 0·07 inch silver strip element.
of new construction.

Fig. 9.—Photographic records of X-ray diffraction tests on silver fuse elements.

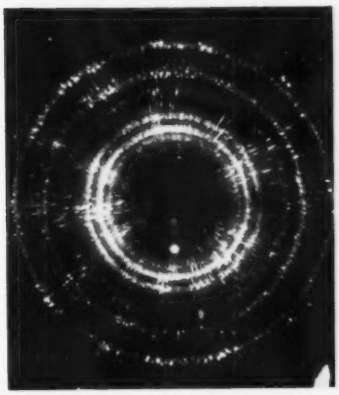

PLATE IV
0·002 inch × 0·07 inch silver strip element.
After 25 years service.

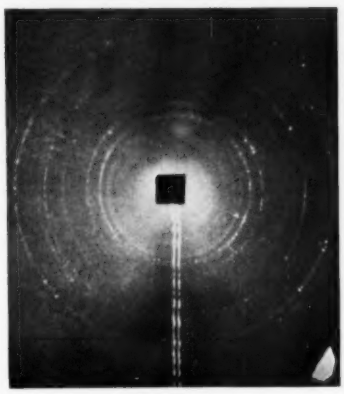

PLATE V
Type 30 silver wire element,
0·022 inch × 0·022 inch.
of new construction.

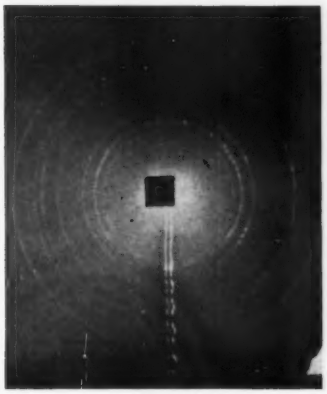

PLATE VI
Type 30 silver wire element,
0·022 inch × 0·022 inch.
After 18 years service.

The plates shown in Fig. 9 are typical of some of the results obtained, and the characteristic patterns appearing may be interpreted as follows : the number and disposition of the concentric rings indicate the crystalline type and structure of the material (silver), the asterism appearing in the form of radial marks indicates the degree of strain within the material, and the continuity or otherwise of the concentric rings indicates grain size. Continuous and unbroken rings appear for fine grain, and broken rings for coarse grain. Plates I and II show slightly greater strain and larger grain size in the old sample than in the new, but this condition seems to be reversed in plates III and IV. Plates V and VI show no apparent difference between the old and new samples.

These tests are not entirely conclusive when considered out of context with the other tests of a more practical nature, but they do show that slight degrees of interior stress and variations in

TABLE 2

MEASUREMENTS OF RESISTANCE

Fuse Links of 16 to 25 Years Service			Similar Fuse Links of New Construction		
Fuse Link Identity Number	Resistance Measured in Microhms	Percentage Variation from Designed Value	Fuse Link Identity Number	Resistance Measured in Microhms	Percentage Variation from Designed Value
ND.100	930	+1·1	ND.200	910	−1·1
ND.101	925	+0·5	ND.201	930	+1·1
ND.102	930	+1·1	ND.202	920	0·0
ND.103	925	+0·5	ND.203	935	+1·6
ND.106	920	0·0	ND.206	900	−2·2
ND.104	910	−1·1	ND.204	910	−1·1
ND.107	920	0·0			
ND.108	960	+4·4			
ND.105	930	+1·1			
ND.109	910	−1·1			
ND.110	214	+4·4	ND.210	200	−2·4
ND.111	212	+3·4	ND.211	197	−3·9
ND.112	190	+3·2	ND.212	184	0·0
			ND.212A	183	−0·55
			ND.212B	182	−1·1
ND.113	205	−3·7	ND.213	219	+2·8
ND.114	209	−1·9	ND.214	220	+3·3
ND.115	208	−2·3	ND.215	220	+3·3
ND.116	182	+1·1	ND.216	176	−2·2
ND.117	182	+1·1	ND.217	175	−2·8
ND.118	182	+1·1	ND.218	173	−3·9
ND.119	147	+0·7	ND.219	143	−2·0
ND.120	141	−3·4	ND.220	143	−2·0
ND.121	144	−1·4	ND.221	145	−0·7
ND.122	142	−2·7	ND.222	143	−2·0
ND.123	140	−4·1	ND.223	145	−0·7
ND.124	153	+4·8	ND.224	148	+1·4
ND.125	148	+1·37			
ND.126	149	+2·0			
ND.127	146	0·0			
ND.128	148	+1·4			
ND.129	151	+3·4			
ND.130	141	−3·4			
ND.131	192	+4·3	ND.231	188	+2·2
ND.132	179	−2·7	ND.232	185	+0·55
ND.133	180	−2·2	ND.233	183	−0·55

grain size are not significant to the proper performances of the fuse. This is shown by the fact that the worst condition detected in the old samples is no worse than the worst condition detected in the new samples. In other words, it is clear that the silver elements of the older fuse links have not suffered change beyond the point where the electrical conductivity is affected.

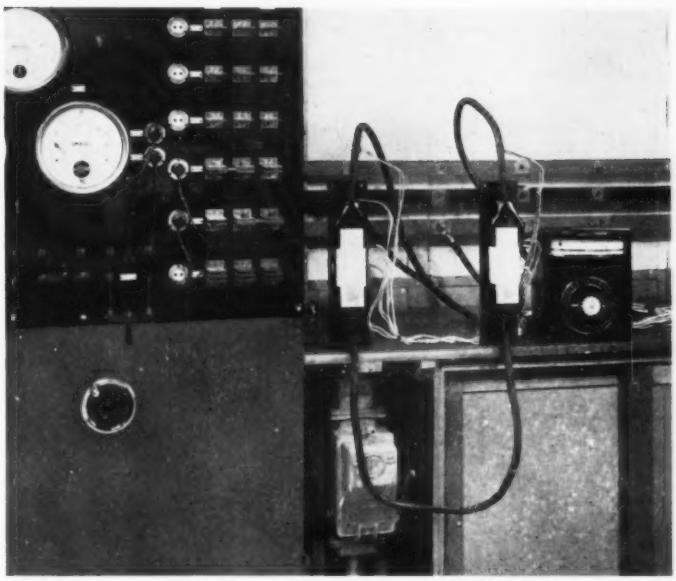

Fig. 10.—*Test rig, showing method of mounting and connecting fuses for temperature rise tests*

Measurements of Fuse Link Resistance

Table 2 shows the values of resistance (in microhms) recorded for a number of the fuses under test. The values for similar fuse links of new construction are also included for comparison. It will be found that in all cases the fuse links fall within the permitted tolerance of + or — 5%. Improved methods of quality control in present-day production make it possible to obtain a higher degree of consistency in resistance values than is indicated by some of the figures in the table. While this fact is not strictly relevant to the objective investigation of non-deterioration, it is necessary to make it clear in order to avoid misconceptions concerning present-day values.

Apart from the fact that the resistance measurements prove that the old fuses are still well within the permitted tolerances allowed under present-day standard specifications, they are necessary as a basis on which to judge the results of temperature rise tests and minimum fusing current tests.

Tests to Determine Temperature Rise Values at Rated Current and to Find the Minimum Fusing Current of the Fuse Links

The maximum temperature rise for various parts of the fuse assembly and the minimum fusing current expressed as a fusing factor are defined for present-day designs of fuse link in B.S. 88 : 1952. The methods used to comply with these requirements were followed in this investigation. Fig. 10 shows the apparatus which was used to obtain the results tabulated in Table 3. It can be seen that the comparisons between the old fuse links and the new fuse links of similar construction are well within the permitted tolerances. Such small divergences as do occur are not incompatible with the physical characteristics of the individual fuse links ; for instance, a slightly lower resistance gives a slightly higher value of minimum fusing current.

The method of carrying out the temperature rise tests is to apply the full rated current to the fuse and to record the actual temperatures of the top fuse contact, top fixed terminal, and a position on the connecting cable approximately 12 inches from the top fuse contact. Readings are taken every 15 minutes and continued until such time as there is no appreciable difference in temperature over three successive readings. Fig. 11 gives in graphical form a typical example of the results of such a test.

The determination of the minimum fusing current is a continuation of the previous test, in which the current is increased by regular steps of 10% the temperature readings being allowed to

TABLE 3

EXAMPLES OF HEATING AND FUSING TESTS

Fuse Link Number		ND.100	ND.200	ND.131	ND.231	ND.124	ND.224
Year Installed		1927	New fuse link of similar construction.	1936	New fuse link of similar construction	1935	New fuse link of similar construction.
Fuse Link Resistance, Microhms		900	920	192	188	153	148
Complete Fuse Resistance, Microhms		1,250	1,200	250	245	248	230
Test Current, Amperes		150	150	300	300	400	400
Temperature rise °C. at rated current.	Top fixed terminal*	34	34	27	26	31	29
	Top fuse terminal†	47	50	37	34	40	36
Ambient Temperature, °C.		20	20	25	25	28‡	28‡
Minimum Fusing Current, Amperes		220	220	420	450	560	600

* Permitted maximum 46°C. in accordance with B.S. 88 : 1952.
† Permitted maximum 55°C. in accordance with B.S. 88 : 1952.
‡ The high ambient temperatures are due to the fact that the tests were carried out on a very hot day in summer.

stabilise for each step before proceeding to the next. This process is continued until the fuse link blows. Fig. 11 also includes a typical example illustrating the methods used.

Short-circuit Tests

As mentioned previously, the short-circuit test was regarded as being the most critical of all. Other electrical tests were mainly concerned with the ability of the fuse to carry load under normal conditions. Under such conditions if deterioration had occurred it would usually result in premature blowing, and although this could cause serious inconvenience it would not involve hazards to personnel or equipment. It is interesting to note that deterioration in a fuse would normally cause it to 'fail to safety' under overload conditions.

The short-circuit test, on the other hand, imposes the maximum strain on the fuse link both electrically and mechanically, and the criterion of success is that the fuse link should interrupt the short-circuit current without bursting or in any way damaging associated equipment.

When an H.R.C. fuse interrupts a heavy fault it exhibits an ability to limit the short-circuit current. This ability is referred to as a 'cut-off' and has the effect of reducing the magnetic and thermal stresses both in the system and within the fuse itself under fault conditions. Cut-off is in fact one of the main reasons why the H.R.C. fuse is so successful as a protective device.

In deciding the tests which should be carried out for non-deterioration it was agreed that a study of cut-off characteristics would provide the most fruitful and critical proofs of possible changes in short-circuit performance due to long service.

The oscillograms shown in Fig. 12 (a, b, c and d) illustrate results of some of the tests. The object of the tests, which were carried out in the Nelson Research Laboratories at Stafford, was to obtain values of cut-off currents and operating times with which to draw an accurate comparison between the old and new fuses of similar construction. It will be seen from the oscillograms that this was achieved by careful control of the test circuit conditions (which were exactly similar to those laid down in B.S. 88 : 1952) and by switching on to the fault at a pre-determined point on the voltage wave in each case.

The resulting current traces obtained show a

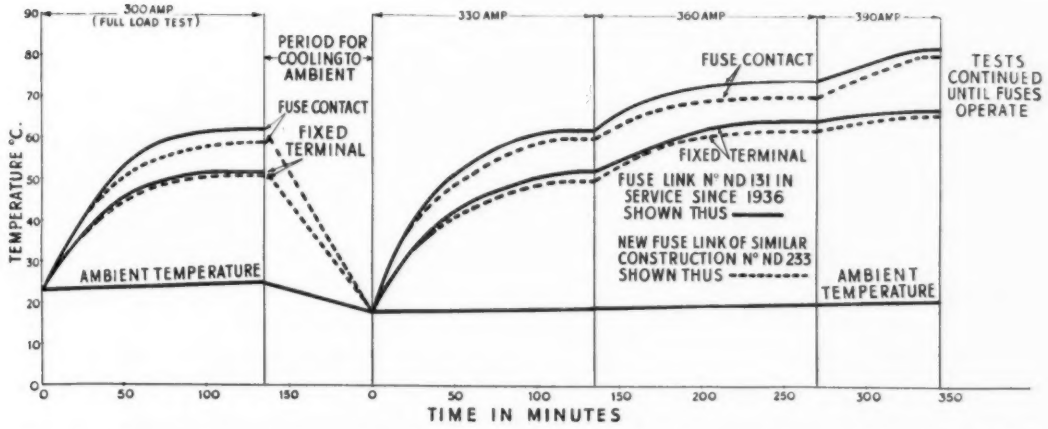

Fig. 11.—*Curves showing comparison between temperature rise characteristics of old and new fuse links of similar construction*

remarkable degree of similarity between the old and the new fuses. Not only is there agreement between the respective peak values and operating times, but the shapes of both the pre-arcing and arcing portion of the traces are similar in characteristic.

It will be seen that two values of prospective short-circuit current were chosen, i.e. 33,000 amp and 16,500 amp, both values being symmetrical R.M.S. and corresponding to British Standard Categories AC4 and AC3 respectively. These values are representative of the most onerous conditions which are likely to have been encountered in service. Typical oscillograms and test data from the actual test reports are shown in Figs. 12a, b, c and d, together with photographs and radiographs showing the condition of the fuse links after successfully interrupting the short-circuit. It is interesting to observe the values of arc voltage shown in the oscillograms. In no case do these exceed the system voltage by more than a small margin, thus illustrating another advantage which is inherent in 'English Electric' H.R.C. fuse protection. The resistance measurements of the blown fuses taken immediately after test leave no doubt that the circuit has been effectively interrupted. The tests were entirely conclusive and in no case was there any evidence of deterioration in respect of the ability of the old fuses to operate under heavy fault conditions.

Non-deterioration in Relation to Present Day Practice

The real value of the foregoing tests is twofold. Firstly, they justify the methods which have been adopted for achieving the highest possible degree of non-deterioration, and confirm objectively what has already been proved in service throughout the world. Secondly, they provide guidance for directing future design policy. New developments in fuse design and new methods of production are constantly being investigated, and every decision concerning them must be ruled by the necessity for maintaining and if possible improving upon established standards.

Non-deterioration is a property which becomes more important as the performance of the fuse is increased. It has been shown that the old fuse links described in the foregoing tests have been able to cope successfully with short-circuit currents up to 33,000 amperes (R.M.S. symmetrical) at normal system voltages. Since they were manufactured, however, the increase in fault levels has called for fuses of higher short-circuit performance. In the case of British Standard 88, the 1947 edition introduced Category AC5 to deal with short-circuit currents up to 46,000 amperes R.M.S. symmetrical, and the Company's range of 'T' type fuses has received certificates of rating by the Association of Short Circuit Testing Authorities for this duty. In Canada a new specification C22.2 No. 106 covering

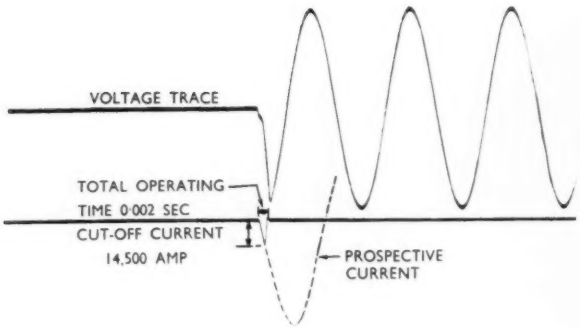

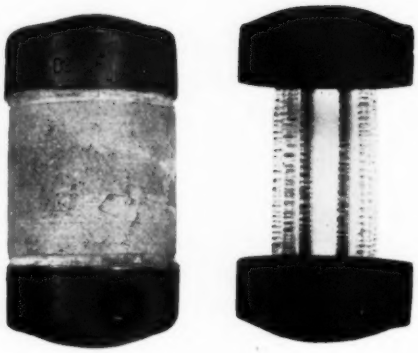

FUSE LINK No. ND106	PROSPECTIVE CURRENT 31·8 kA.	TOTAL OPERATING TIME	0·002 SEC.
TYPE D2OOF.	PEAK CURRENT – – 62·2 kA.	PRE-ARCING TIME – –	0·001 SEC.
YEAR INSTALLED, 1927	CUT-OFF CURRENT – 14·5 kA.	ARCING TIME – –	0·001 SEC.

RESISTANCE ACROSS FUSE AFTER TEST—38·0 MEGOHMS

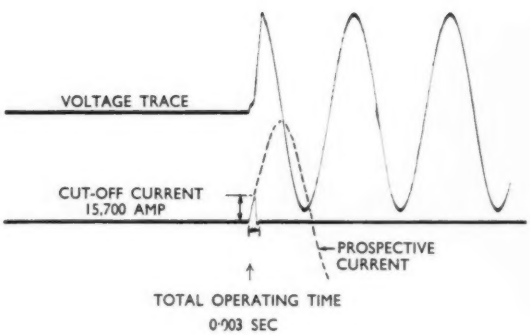

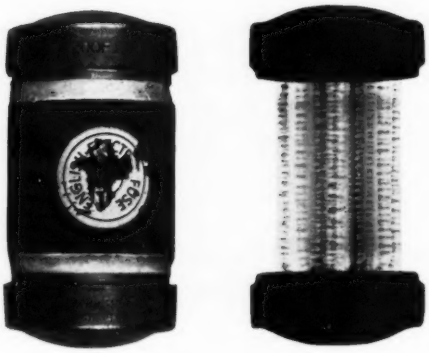

FUSE LINK No. ND256	PROSPECTIVE CURRENT 32·2 kA.	TOTAL OPERATING TIME	0·003 SEC.
TYPE D200F.	PEAK CURRENT – – 62·2 kA.	PRE-ARCING TIME – –	0·001 SEC.
YEAR INSTALLED, NEW	CUT-OFF CURRENT – 15·7 kA.	ARCING TIME – –	0·002 SEC.

RESISTANCE ACROSS FUSE AFTER TEST—3.0 MEGOHMS

Fig. 12a.—*Short-circuit tests at* 33 *kA to compare cut-off characteristics of old and new fuses of similar construction*

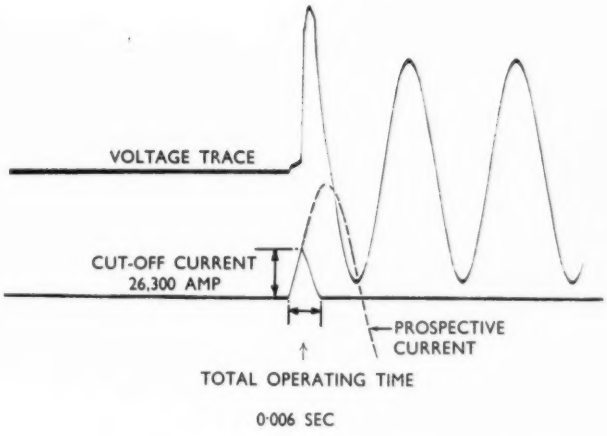

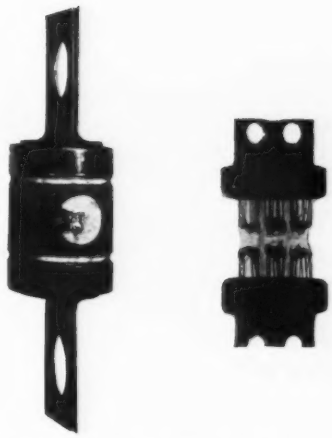

FUSE LINK No. ND112	PROSPECTIVE CURRENT 31·8 kA.	TOTAL OPERATING TIME	0·006 SEC.
TYPE 28TK, 300 AMP	PEAK CURRENT – – 62·2 kA.	PRE-ARCING TIME – –	0·002 SEC.
YEAR INSTALLED, 1934	CUT-OFF CURRENT – 26·3 kA.	ARCING TIME – –	0·004 SEC.

RESISTANCE ACROSS FUSE AFTER TEST—15·0 MEGOHMS

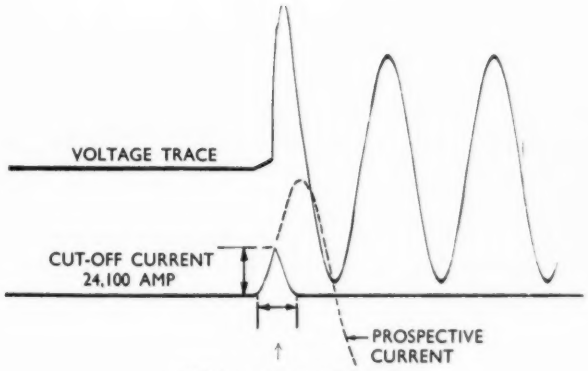

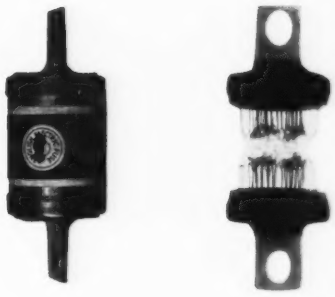

FUSE LINK No. ND257	PROSPECTIVE CURRENT 32·1 kA.	TOTAL OPERATING TIME	0·005 SEC.
TYPE TKF, 300 AMP	PEAK CURRENT – – 62·2 kA.	PRE-ARCING TIME – –	0·002 SEC.
YEAR INSTALLED, NEW	CUT-OFF CURRENT – 26·0 kA.	ARCING TIME – –	0·003 SEC.

RESISTANCE ACROSS FUSE AFTER TEST—100·0 MEGOHMS

Fig. 12b.—*Short-circuit tests at* 33 *kA to compare cut-off characteristics of old and new fuses of similar construction*

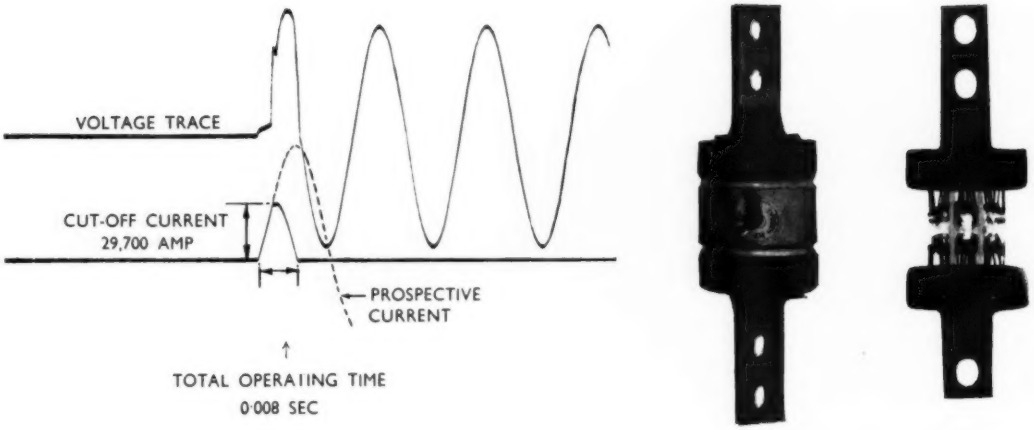

FUSE LINK No. ND126	PROSPECTIVE CURRENT 32·1 kA.	TOTAL OPERATING TIME	0·008 SEC.
TYPE TM, 400 AMP	PEAK CURRENT - - 62·2 kA.	PRE-ARCING TIME - -	0·003 SEC.
YEAR INSTALLED, 1935	CUT-OFF CURRENT - 29·7 kA.	ARCING TIME - -	0·005 SEC.

RESISTANCE ACROSS FUSE AFTER TEST—15·0 MEGOHMS

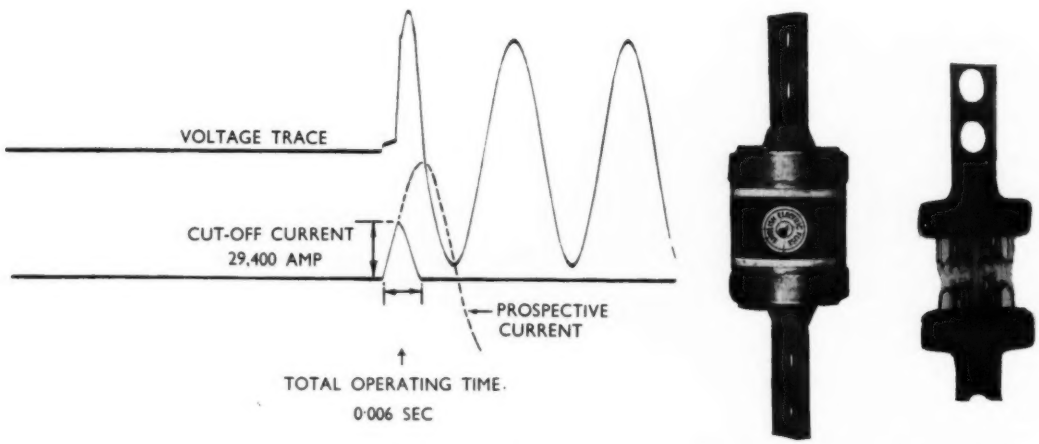

FUSE LINK No. ND258	PROSPECTIVE CURRENT 31·7 kA.	TOTAL OPERATING TIME	0·006 SEC.
TYPE TM, 400 AMP	PEAK CURRENT - - 62·2 kA.	PRE-ARCING TIME - -	0·003 SEC.
YEAR INSTALLED, NEW	CUT-OFF CURRENT - 29·4 kA.	ARCING TIME - -	0·003 SEC.

RESISTANCE ACROSS FUSE AFTER TEST—1·5 MEGOHMS

Fig. 12c.— *Short-circuit tests at* 33 *kA to compare cut-off characteristics of old and new fuses of similar construction*

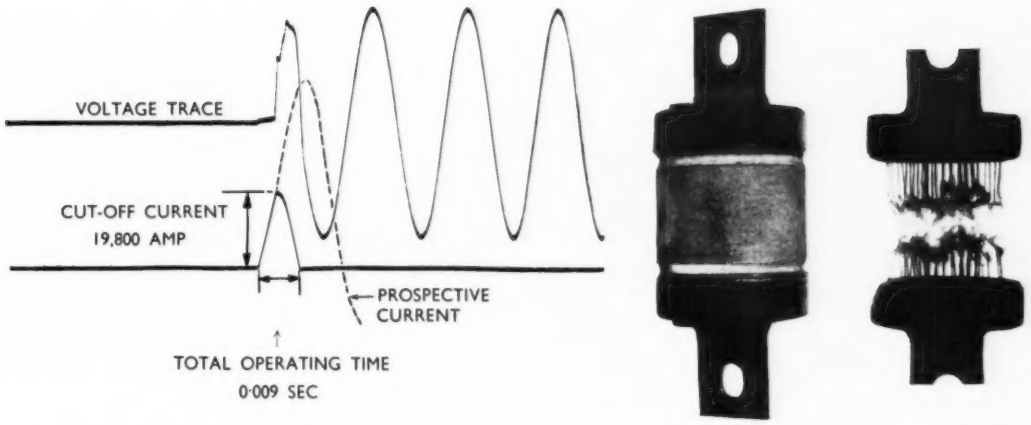

FUSE LINK No. ND132	PROSPECTIVE CURRENT 16·4 kA.	TOTAL OPERATING TIME	0·009 SEC.
TYPE TKF, 300 AMP	PEAK CURRENT - - 49·8 kA.	PRE-ARCING TIME - -	0·003 SEC.
YEAR INSTALLED, 1936	CUT-OFF CURRENT - 19·8 kA.	ARCING TIME - -	0·006 SEC.

RESISTANCE ACROSS FUSE AFTER TEST—100·0 MEGOHMS

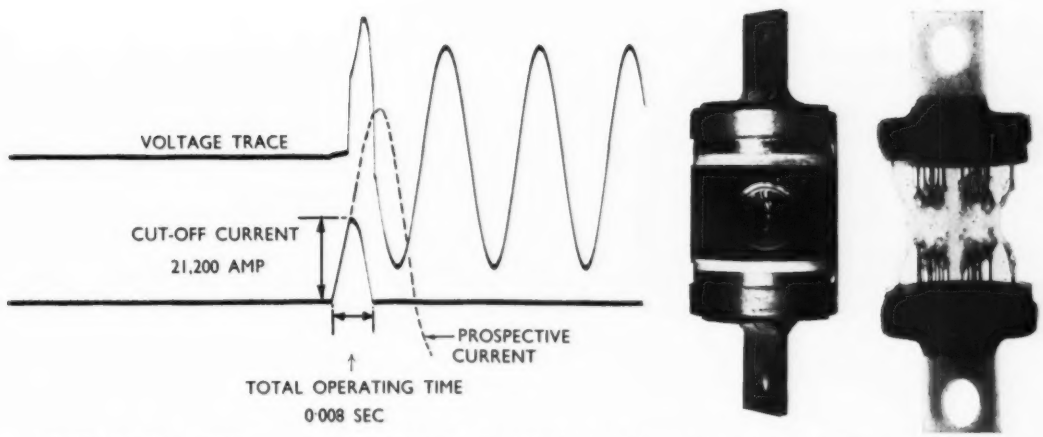

FUSE LINK No. ND252	PROSPECTIVE CURRENT 16·7 kA.	TOTAL OPERATING TIME	0·008 SEC.
TYPE TKF, 300 AMP	PEAK CURRENT - - 49·8 kA.	PRE-ARCING TIME - -	0·003 SEC.
YEAR INSTALLED, NEW	CUT-OFF CURRENT - 21·2 kA.	ARCING TIME - -	0·005 SEC.

RESISTANCE ACROSS FUSE AFTER TEST—100·0 MEGOHMS

Fig. 12d.—*Short-circuit tests at* 16.5 *kA to compare cut-off characteristics of old and new fuses of similar construction*

H.R.C. fuses calls for still higher rupturing capacity, namely 100,000 amperes R.M.S. assymmetrical (corresponding to 80,000 amperes R.M.S. symmetrical) at 600 volts A.C. The Company has designed a new range of fuses, Type 'C', which have been successfully tested for this duty and have received Approval No. 12203 from the Canadian Standards Association.

The tests for non-deterioration also provided valuable evidence in another direction. All specifications and proving tests pre-suppose that the manufacturer will produce equipment for general sale which is faithful in every respect to declared characteristics and identical with the samples which have successfully passed the prescribed tests. This is especially important in the case of the cartridge fuse link, because its functioning parts are totally enclosed and cannot be inspected. Its success as a protective device depends entirely upon its soundness of design and the skill by which it is manufactured. In view of this the reputable manufacturer is obliged to adopt techniques which leave no doubt that each fuse produced will perform in accordance with accepted specifications.

The question of consistency in manufacture and performance is constantly under review in this Company, and in addition to taking resistance measurements of every fuse manufactured, tests are continually in progress to check consistency under normal service and fault conditions. The result of this is that a high degree of consistency has been achieved on every fuse and range of fuses manufactured. The tests for non-deterioration now prove that this consistency can in fact be maintained throughout the life of the fuse.

Although the samples chosen for test were taken from a public supply network, the results obtained apply equally to other applications. H.R.C. fuses are used extensively in industrial, marine, traction, and aircraft installations, and the requirements of non-deterioration are equally valid to them all.

THE
ENGLISH ELECTRIC
COMPANY LIMITED

ALLIED AND ASSOCIATED COMPANIES

English Electric Export and Trading Company Ltd

English Electric Valve Company Ltd

D. Napier & Son Ltd

Marconi's Wireless Telegraph Company Ltd
and its Subsidiaries

The Marconi International Marine Communication Company Ltd
and its Subsidiaries

Canadian Marconi Company

John Inglis Company Ltd, Toronto

English Electric Company of Canada Ltd

The English Electric Company of South Africa (Proprietary) Ltd

The Power and Traction Finance Company Ltd

Associated British Manufacturers (Egypt) Ltd

PRODUCTS OF THE ENGLISH ELECTRIC COMPANY LIMITED

Generating Plant—Steam, Hydraulic, Gas Turbine or Diesel. Transformers, Rectifiers and Switchgear. Industrial Electrification. Electric and Diesel-electric Traction. Marine Propulsion and Auxiliaries. Aircraft. Aircraft Electrical Equipment. Industrial Electronic Equipment. Instruments. Domestic Electrical Appliances. Television Receivers.